

This is an Open Access document downloaded from ORCA, Cardiff University's institutional repository: <https://orca.cardiff.ac.uk/id/eprint/114243/>

This is the author's version of a work that was submitted to / accepted for publication.

Citation for final published version:

Andrew, Carrie, Halvorsen, Rune, Heegaard, Einar, Kuyper, Thomas W., Heilmann-Clausen, Jacob, Krisai-Greilhuber, Irmgard, Bässler, Claus, Egli, Simon, Gange, Alan C., Høiland, Klaus, Kirk, Paul M., Senn-Irlet, Beatrice, Boddy, Lynne, Büntgen, Ulf and Kauserud, Håvard 2018. Continental-scale macrofungal assemblage patterns correlate with climate, soil carbon and nitrogen deposition. *Journal of Biogeography* 45 (8), pp. 1942-1953. 10.1111/jbi.13374

Publishers page: <http://dx.doi.org/10.1111/jbi.13374>

Please note:

Changes made as a result of publishing processes such as copy-editing, formatting and page numbers may not be reflected in this version. For the definitive version of this publication, please refer to the published source. You are advised to consult the publisher's version if you wish to cite this paper.

This version is being made available in accordance with publisher policies. See <http://orca.cf.ac.uk/policies.html> for usage policies. Copyright and moral rights for publications made available in ORCA are retained by the copyright holders.



1 Continental-scale macro-fungal assemblage patterns correlate with climate, soil carbon and  
2 nitrogen deposition

3  
4  
5  
6  
7  
8  
9 Authors:

10 Carrie Andrew, Rune Halvorsen, Einar Heegaard, Thomas W Kuyper, Jacob Heilmann-  
11 Clausen, Irmgard Krisai-Greilhuber, Claus Bässler, Simon Egli, Alan C Gange, Klaus  
12 Høiland, Paul M Kirk, Beatrice Senn-Irlet, Lynne Boddy, Ulf Büntgen, Håvard Kauserud

13  
14  
15  
16  
17  
18  
19  
20 Affiliations:

21  
22 **CA** (corresponding author) ([carrie.andrew@wsl.ch](mailto:carrie.andrew@wsl.ch)), Swiss Federal Research Institute WSL,  
23 CH-8903 Birmensdorf, Switzerland; (2nd affiliation:) University of Cambridge, Department  
24 of Geography, CB2 3EN, UK; (3rd affiliation:) Section for Genetics and Evolutionary  
25 Biology (EVOGENE), University of Oslo, Blindernveien 31, 0316 Oslo, Norway

26  
27  
28  
29 **RH** ([rune.halvorsen@nhm.uio.no](mailto:rune.halvorsen@nhm.uio.no)), Department of Research and Collections, Natural History  
30 Museum, University of Oslo, NO-0318 Oslo, Norway

31  
32  
33  
34 **EH** ([fmroehe@fylkesmannen.no](mailto:fmroehe@fylkesmannen.no)), Forestry and Forest Resources, Norwegian Institute of  
35 Bioeconomy Research, Fanaflaten 4, N-5244 Fana, Norway

36  
37  
38  
39 **TWK** ([thom.kuyper@wur.nl](mailto:thom.kuyper@wur.nl)), Department of Soil Quality, Wageningen University, PO Box  
40 47, 6700 AA Wageningen, The Netherlands

41  
42  
43  
44 **JHC** ([jheilmann-clausen@snm.ku.dk](mailto:jheilmann-clausen@snm.ku.dk)), Centre for Macroecology, Evolution and Climate,  
45 Natural History Museum of Denmark, University of Copenhagen, DK-2100 Copenhagen,  
46 Denmark

47  
48  
49  
50 **IKG** ([irmgard.greilhuber@univie.ac.at](mailto:irmgard.greilhuber@univie.ac.at)), Department of Botany and Biodiversity Research,  
51 University of Vienna, A-1030 Vienna, Austria

52  
53  
54  
55  
56  
57  
58  
59  
60

- 1  
2  
3 25 **CB** ([Claus.Baessler@npv-bw.bayern.de](mailto:Claus.Baessler@npv-bw.bayern.de)), Bavarian Forest National Park, Freyunger Str. 2, D-  
4  
5 26 94481 Grafenau, Germany; (2nd affiliation:) Technical University of Munich, Chair for  
6  
7 27 Terrestrial Ecology, Hans-Carl-von-Carlowitz-Platz 2, 85354 Freising, Germany  
8  
9 28 **SE** ([simon.egli@wsl.ch](mailto:simon.egli@wsl.ch)), Swiss Federal Research Institute WSL, CH-8903 Birmensdorf,  
10  
11 29 Switzerland  
12  
13 30 **ACG** ([a.gange@rhul.ac.uk](mailto:a.gange@rhul.ac.uk)), School of Biological Sciences, Royal Holloway, University of  
14  
15 31 London, Egham, Surrey TW20 0EX, UK  
16  
17 32 **KH** ([klaus.hoiland@ibv.uio.no](mailto:klaus.hoiland@ibv.uio.no)), Section for Genetics and Evolutionary Biology  
18  
19 33 (EVOGENE), University of Oslo, Blindernveien 31, 0316 Oslo, Norway  
20  
21 34 **PMK** ([P.Kirk@kew.org](mailto:P.Kirk@kew.org)), Mycology Section, Jodrell Laboratory, Royal Botanic Garden,  
22  
23 35 Kew, Surrey TW9 3DS, UK  
24  
25 36 **BSI** ([beatrice.senn@wsl.ch](mailto:beatrice.senn@wsl.ch)), Swiss Federal Research Institute WSL, CH-8903 Birmensdorf,  
26  
27 37 Switzerland  
28  
29 38 **LB** ([BoddyL@cardiff.ac.uk](mailto:BoddyL@cardiff.ac.uk)), School of Biosciences, Cardiff University, Sir Martin Evans  
30  
31 39 Building, Museum Avenue, Cardiff CF10 3AX, UK  
32  
33 40 **UB** ([ulf.buentgen@geog.cam.ac.uk](mailto:ulf.buentgen@geog.cam.ac.uk)), University of Cambridge, Department of Geography,  
34  
35 41 CB2 3EN, UK; (second affiliation:) Swiss Federal Research Institute WSL, CH-8903  
36  
37 42 Birmensdorf, Switzerland; (third affiliation:) Global Change Research Centre and Masaryk  
38  
39 43 University, 613 00 Brno, Czech Republic  
40  
41 44 **HK** ([havard.kauserud@ibv.uio.no](mailto:havard.kauserud@ibv.uio.no)), Section for Genetics and Evolutionary Biology  
42  
43 45 (EVOGENE), University of Oslo, Blindernveien 31, 0316 Oslo, Norway  
44  
45 46  
46  
47 47 Keywords (6-10): Assemblage, Biogeography, Climate, Ectomycorrhizal, Europe, Fungi,  
48  
49 48 Macroecology, Saprotrophic, Temporal change  
50  
51  
52  
53  
54  
55 49  
56  
57  
58  
59  
60

1  
2  
3  
4  
5  
6  
7  
8  
9  
10  
11  
12  
13  
14  
15  
16  
17  
18  
19  
20  
21  
22  
23  
24  
25  
26  
27  
28  
29  
30  
31  
32  
33  
34  
35  
36  
37  
38  
39  
40  
41  
42  
43  
44  
45  
46  
47  
48  
49  
50  
51  
52  
53  
54  
55  
56  
57  
58  
59  
60

50 Running-title: Fungal assemblages across Europe

For Peer Review

1  
2  
3 51 Abstract:

4  
5 52 **Aim** Macroecological scales of species compositional trends are well documented for a  
6  
7 53 variety of plant and animal groups, but remain sparse for fungi, despite their ecological  
8  
9 54 importance in carbon and nutrient cycling. It is, thus, essential to understand the composition  
10  
11 55 of fungal assemblages across broad geographical scales, and the underlying drivers. Our  
12  
13 56 overall aim was to describe these patterns for fungi across two nutritional modes  
14  
15 57 (saprotrophic and ectomycorrhizal). Furthermore, we aimed to elucidate the temporal  
16  
17 58 component of fruiting patterns and to relate these to soil carbon and nitrogen deposition.  
18  
19

20 59 **Location** Central and northern Europe

21  
22 60 **Methods** 4.9 million fungal fruit body observations throughout Europe, collected between  
23  
24 61 1970–2010, were analyzed to determine the two main environmental and geographical  
25  
26 62 gradients structuring fungal assemblages for two main nutritional modes, saprotrophic and  
27  
28 63 ectomycorrhizal fungi.  
29

30  
31 64 **Results** Two main gradients explaining the geography of compositional patterns were  
32  
33 65 identified, for each nutritional mode. Mean annual temperature (and related collinear,  
34  
35 66 seasonal measures) correlated most strongly with the first gradient for both nutritional modes.  
36  
37 67 Soil organic carbon was the highest correlate of the second compositional gradient for  
38  
39 68 ectomycorrhizal fungi, suspected as an indicator of vegetation- and pH-related covariates. In  
40  
41 69 contrast, nitrogen deposition constituted a second gradient for saprotrophic fungi, likely a  
42  
43 70 proxy for anthropogenic pollution. Compositional gradients and environmental conditions  
44  
45 71 correlated similarly when the data were divided into two time intervals of 1970–1990 and  
46  
47 72 1991–2010. Evidence of compositional temporal change was highest with increasing altitude  
48  
49 73 and latitude.  
50

51  
52 74 **Main conclusions** Fungal assemblage patterns demonstrate clear biogeographical patterns  
53  
54 75 that relate the nutritional modes to their main environmental correlates of temperature, soil  
55  
56  
57  
58  
59  
60

1  
2  
3 76 organic carbon and nitrogen deposition. With respect to global change impacts, the highest  
4  
5 77 rates of compositional change by time suggest targeting higher latitudes and altitudes for a  
6  
7 78 better understanding of fungal dynamics. We, finally, suggest further examination of the  
8  
9 79 ranges and dispersal abilities of fungi to better assess responses to global change.  
10  
11  
12  
13  
14  
15  
16  
17  
18  
19  
20  
21  
22  
23  
24  
25  
26  
27  
28  
29  
30  
31  
32  
33  
34  
35  
36  
37  
38  
39  
40  
41  
42  
43  
44  
45  
46  
47  
48  
49  
50  
51  
52  
53  
54  
55  
56  
57  
58  
59  
60

For Peer Review

1  
2  
3 80 Biosketch  
4

5 81 Carrie Andrew has been responsible for preparing the manuscript, and for many of the  
6  
7 82 analyses conducted with, the data utilized here, and as is better described in Andrew et al.  
8  
9 83 2017 (where original data sources and contact / website information are listed). Dr. Andrew  
10  
11 84 was a postdoctoral researcher for the duration of this project. The work presented in this  
12  
13 85 manuscript represents a component of the ClimFun project, an international collaboration that  
14  
15 86 united national-scale fruit body datasets for the purposes of macroecological investigations of  
16  
17 87 fungi in relation to environmental drivers, especially global change components. Author  
18  
19 88 contributions are: HK, CA and EH, conceived the main ideas; CA prepared the data with data  
20  
21 89 access and rights provided via ACG, BSI, CB, IKG, JHC, PMK, SE, and TWK; CA, RH and  
22  
23 90 EH analysed the data; CA led the writing; and all co-authors contributed to wide-range  
24  
25 91 general discussion and interpretation during the project, along with manuscript edits: RH, EH,  
26  
27 92 TWK, JHC, IKG, CB, SE, ACG, KH, PMK, BSI, LB, UB, and HK.  
28  
29  
30

31 93

32  
33 94 Introduction  
34

35 95 Detecting and understanding broad-scale geographic patterns of organisms is a critically  
36  
37 96 important issue in global change research. Patterns of fungal species assemblage distributions  
38  
39 97 have rarely been considered in macroecology, despite the key contributions that fungi make to  
40  
41 98 ecosystem processes (Heilmann-Clausen, Barron, et al. 2014). There are two major functional  
42  
43 99 guilds of fungi that produce macroscopic fruit bodies, based on nutritional mode (i.e.,  
44  
45 100 saprotrophic fungi that feed on dead organic matter, and ectomycorrhizal fungi that are  
46  
47 101 mutualistic root symbionts), and each is crucial to ecosystem functioning. It is, thus,  
48  
49 102 important to identify any differences in their geographic patterns, and changes in these,  
50  
51 103 especially in relation to global change.  
52  
53

54  
55 104  
56  
57  
58  
59  
60

1  
2  
3 105 In terms of the known biogeographic patterns of fungi, mycorrhizal fungal species are  
4  
5 106 strongly coupled to their host plants' ranges and climate regions (Tedersoo et al. 2012;  
6  
7 107 Tedersoo, Bahram, Pölmé, et al. 2014). Much research has focused on this connection, to the  
8  
9 108 point of extrapolating biotic trends as a means to describe matching, un-surveyed fungal  
10  
11 109 patterns (Soudzilovskaia et al. 2015; Swaty Michael, Deckert & Gehring 2016; Bueno et al.  
12  
13 110 2017). Saprotrophic fungi, also, are often considered in terms of their substrates, and their  
14  
15 111 distribution often reflects the availability and quality of specific substrates, e.g., wood types  
16  
17 112 and leaf litter (Bässler, Müller, Dziöck & Brandl 2010; Heilmann-Clausen, Aude, et al. 2014).  
18  
19 113 Gaps still exist in terms of knowledge of their overall distribution patterns, as well as the  
20  
21 114 abiotic processes that likely determine their distributions.  
22  
23  
24  
25

26 116 The scattered representations of fungal biogeography studies to date have most often  
27  
28 117 extrapolated low but sequence-deep sample intensities (small grain sizes) across large  
29  
30 118 geographical extents, due to the limitations of molecular-based sampling approaches  
31  
32 119 (Unterseher et al. 2011). This 'necessary evil' that leaves gaps in our knowledge of fungal  
33  
34 120 distributions in space and time. The related fungal community gradients, then, are not  
35  
36 121 continuously represented (due to low density of geographical samples) and, instead, capture  
37  
38 122 categorical levels of what are actually continuous patterns of variation.  
39  
40  
41  
42

43 124 The taxonomic coverage across studies can also limit extrapolations. While sequences are  
44  
45 125 identified to operational taxonomic units approximating species (Meiser, Bálint & Schmitt  
46  
47 126 2014; Taylor et al. 2014), studies have often focused on specific families or genera to benefit  
48  
49 127 phylogenetic knowledge (i.e., Naff, Darcy & Schmidt 2013; Tedersoo, Bahram, Ryberg, et al.  
50  
51 128 2014). Other studies have focused on higher-level taxa of bacteria or fungi (Martiny et al.  
52  
53 129 2006). Although previous studies have suggested, expectedly, that fungal communities  
54  
55  
56  
57  
58  
59  
60

1  
2  
3 130 arrange along environmental and geographical gradients, this pattern is yet to be clearly  
4  
5 131 investigated.

6  
7 132

8  
9 133 In Europe, extensive fungal fruit body records have been catalogued at the largest  
10  
11 134 spatiotemporal scales currently available (Andrew et al. 2017). While records with  
12  
13 135 comprehensive sampling distributions that span multiple decades make it possible to  
14  
15 136 investigate temporal changes of fungi related to climate, such data sets have so far mainly  
16  
17 137 been used for studying phenology (e.g., Kauserud et al. 2008; Kauserud et al. 2010; Buntgen,  
18  
19 138 Kauserud & Egli 2012; Kauserud et al. 2012; Boddy et al. 2014). The uniform coverage of  
20  
21 139 fungal species data throughout a large part of their geographical extent (Andrew et al. 2017),  
22  
23 140 when aggregated at appropriate spatial resolutions and across decades of time, sets this data  
24  
25 141 source apart from molecular-based data. These data capture the entirety of fungal  
26  
27 142 environmental and geographical gradients more completely than current molecular data, and  
28  
29 143 in this respect, are ideal sources to better understand environmental correlates to fungal  
30  
31 144 biogeography.  
32  
33  
34

35 145

36  
37 146 It is this large spatiotemporal range of multisource fungal records data collected in varied  
38  
39 147 manners, combined with booming additions through citizen science projects (e.g., Halme,  
40  
41 148 Heilmann-Clausen, Rämä, Kosonen & Kunttu 2012; Heilmann-Clausen, Barron, et al. 2014),  
42  
43 149 that counteracts other limitations of fruit body data. Although the records focus almost  
44  
45 150 exclusively on macro-fungi i.e., fungi that form conspicuous fruit bodies, both above and  
46  
47 151 belowground, these include many of the ecologically most significant groups. For example,  
48  
49 152 habitat preference in wood-decomposing fungi and the decay they cause are well, if not  
50  
51 153 completely, captured with fruit body records (e.g., Heilmann-Clausen et al. 2016). While  
52  
53 154 sporadic and ephemeral fruiting patterns of fungi can limit the accuracy of their  
54  
55  
56  
57  
58  
59  
60

1  
2  
3 155 representation, the problem is minimized by compiling data across multiple years and at  
4  
5 156 broader spatial resolutions than original point observations (Andrew et al. 2017). Finally,  
6  
7 157 presence-only data for fruit bodies are the sole source of large-scale historical-to-  
8  
9 158 contemporary records in mycology. Thus, fruit body records offer unique ecological  
10  
11 159 information that may open up new insights into the effects of global change on fungi. Due to  
12  
13 160 the high spatiotemporal resolution and extent, they serve as a foundation to build upon for  
14  
15 161 biogeographical and macroecological research in mycology.  
16  
17  
18 162

19  
20 163 In this study, we use 4.9 million fruit body occurrences, extracted from a large-scale,  
21  
22 164 European meta-database with more than 6 million fungal fruit body records (Andrew et al.  
23  
24 165 2017), to identify the major fungal biogeographic compositional patterns in Europe. For fungi  
25  
26 166 in two main nutritional modes, saprotrophic and ectomycorrhizal, we first identified the  
27  
28 167 gradients structuring assemblages and their environmental correlates. We next investigated  
29  
30 168 differences in fungal compositional patterns between two equal time periods, 1970–1990 and  
31  
32 169 1991–2010, for each nutritional mode. In particular, we searched for geographical regions  
33  
34 170 with greater compositional change, and for the overall environmental drivers that correlated  
35  
36 171 with any compositional shift. As most knowledge in the field is untested, we adopted an  
37  
38 172 inductive, hypothesis-generating approach, i.e., not to formulate specific hypotheses beyond a  
39  
40 173 general expectation that the climate and environment (e.g., nitrogen deposition) that structures  
41  
42 174 plant and fungal compositions at smaller scales will likely similarly structure macro-scale  
43  
44 175 fungal assemblages. From our results, we generate biogeographical and macroecological  
45  
46 176 hypotheses related to fungi, and suggest topics for further research.  
47  
48  
49  
50 177

51  
52 178 Methods

53  
54 179 Fungal data  
55  
56  
57  
58  
59  
60

1  
2  
3 180 This study utilized data from a component of the ClimFun ‘meta-database,’ a set of unified,  
4  
5 181 multi-source data which originated from many, independent data repositories of fungal  
6  
7 182 fruiting records across Europe (Andrew et al. 2017). The data are comprehensive in temporal  
8  
9 183 and spatial coverage, extending decades into the past and covering a large geographic range  
10  
11 184 of Europe. Given the large temporal and spatial coverage of the data, they are a reliable  
12  
13 185 source for answering questions in macroecology. These data have been shown to be especially  
14  
15 186 robust to large-scale phenology analyses (Andrew et al. 2018), demonstrating their potential  
16  
17 187 for biogeographical studies such as here. Earlier bias removal techniques included  
18  
19 188 harmonization of nomenclature, removal of out-of-country records, removal of data with  
20  
21 189 inconsistent or incomplete date records, removal of duplicate records, and other techniques  
22  
23 190 standard for formatting these types of data formatting. Due to the large amount of records,  
24  
25 191 these processes did not greatly affect the overall, final amounts (e.g., Andrew et al. 2017).  
26  
27  
28  
29

30  
31 193 National-scale data in the ClimFun meta-database with a substantial amount of records (i.e.,  
32  
33 194 Austria, Denmark, Germany, Netherlands, Norway, Slovenia, Switzerland, and the United  
34  
35 195 Kingdom) were selected across a timespan from 1970 to 2010, for which data were more  
36  
37 196 reliable due to less recording bias than earlier time periods, and also was temporally robust,  
38  
39 197 ensuring stability in climate values (as opposed to interannual weather variability). Species  
40  
41 198 were restricted to the macroscopic fruit body forming Agaricomycotina (the classes  
42  
43 199 Agaricomycetes, Tremellomycetes and Dacrymycetes; including fungi with flattened fruit  
44  
45 200 bodies on wood and soil (corticoid fungi)), as other taxonomic groups comprised very low  
46  
47 201 proportions of the records (Andrew et al. 2017) and, at this spatiotemporal scale, were highly  
48  
49 202 biased in terms of under-collection and sampling bias. Taxa were assigned to their dominant  
50  
51 203 nutritional mode based on Rinaldi, Comandini & Kuyper (2008), Tedersoo and Smith (2013),  
52  
53 204 and with additional species-specific information added through expertise (nutritional mode  
54  
55  
56  
57  
58  
59  
60

1  
2  
3 205 data compiled 2016 by K. Høiland, University of Oslo, Norway, with additional aid from: B.  
4  
5 206 Senn-Irlet, J. Heilmann-Clausen, A. C. Gange, L. Boddy, S. Egli, T. W. Kuyper, I. Krisai-  
6  
7 207 Greilhuber). The number of records varied between nutritional modes, as did the grid cell  
8  
9 208 representation for each guild (see all results figures to compare between time period amounts  
10  
11 209 and nutritional modes), with greater coverage by saprotrophic fungi.

12  
13 210

#### 14 15 211 Environmental data

16  
17 212 Available environmental variables were gridded at the  $50 \times 50$  km level after connecting the  
18  
19 213 ClimFun records data in earlier steps to open-source metadata at their highest available  
20  
21 214 resolutions (i.e., geographical points), thus gaining the most precision possible in terms of  
22  
23 215 fruiting records and their associated environment. Environmental data were obtained and  
24  
25 216 formatted from each of the following open-data sources: Climate and altitude data were  
26  
27 217 extracted at the 2.5 and 0.5 minute resolution, respectively (equivalent to approximately 4.5  
28  
29 218 and 1 km at the equator), from WorldClim (<http://www.worldclim.org>; Hijmans, Cameron,  
30  
31 219 Parra, Jones & Jarvis 2005). GIMMS AVHRR Global NDVI-3g (Normalized Difference  
32  
33 220 Vegetation Index) data with 1/12-degree resolution (approximately 9.5 km at the equator) was  
34  
35 221 extracted from Ecocast (<https://ecocast.arc.nasa.gov>). The average of annual averages of  
36  
37 222 monthly mean value concatenated climate data composites for the period 1982–2010 was  
38  
39 223 used. NDVI corresponds to the start of spring in northern latitudes and is thus often used as a  
40  
41 224 measure of initial primary productivity (Pettorelli et al. 2005; Nielsen et al. 2012). Percent  
42  
43 225 soil organic carbon was extracted from the OCTOP (Topsoil Organic Carbon Content for  
44  
45 226 Europe) dataset, from the Joint Research Centre - European Soil Data Centre (ESDAC), with  
46  
47 227 1 km original resolution ([http://esdac.jrc.ec.europa.eu/content/octop-topsoil-organic-carbon-](http://esdac.jrc.ec.europa.eu/content/octop-topsoil-organic-carbon-content-europe)  
48  
49 228 [content-europe](http://esdac.jrc.ec.europa.eu/content/octop-topsoil-organic-carbon-content-europe)). Reduced and oxidised nitrogen deposition data were obtained from  
50  
51 229 Greenhouse Gas Management in European land use systems (GHG Europe) FP7, using 0.25  
52  
53  
54  
55  
56  
57  
58  
59  
60

1  
2  
3 230 degree (approximately 27-28 km at the equator) NCAR CTM data ([http://www.europe-](http://www.europe-fluxdata.eu/ghg-europe/data/others-data)  
4  
5 231 [fluxdata.eu/ghg-europe/data/others-data](http://www.europe-fluxdata.eu/ghg-europe/data/others-data)). Finally, land cover was extracted from the  
6  
7 232 European Environment Agency (EEA) Corine Land Cover (CLC) 2006 raster data (version  
8  
9 233 17) with an original 100 m resolution ([http://www.eea.europa.eu/data-and-maps/data/corine-](http://www.eea.europa.eu/data-and-maps/data/corine-land-cover-2006-raster-3)  
10  
11 234 [land-cover-2006-raster-3](http://www.eea.europa.eu/data-and-maps/data/corine-land-cover-2006-raster-3)). While data with varying spatial resolutions is not ideal, this issue  
12  
13 235 was balanced against utilizing data with the best temporal resolution matching the fungal  
14  
15 236 recordings, as well as the ability to find and extract data for each covariate.  
16  
17  
18 237

19  
20 238 To minimize multicollinearity, pairwise Pearson correlation coefficients between all potential  
21  
22 239 environmental covariates were calculated (Appendix S1) and variables with a coefficient  
23  
24 240 below a threshold of 0.60 (absolute value) were retained (cf. Dormann et al. 2013). Total and  
25  
26 241 seasonal precipitation were positively correlated, as were annual, seasonal and ranges in  
27  
28 242 temperature. In the case of temperature, the latter two were positively correlated with easting  
29  
30 243 (longitude) and were thus not retained. Nitrogen deposition (both  $\text{NH}_x$ , and  $\text{NO}_y$ ) was  
31  
32 244 correlated with northing (negative) and easting (positive).  $\text{NH}_x$  was selected for further  
33  
34 245 analyses, serving also as a proxy for  $\text{NO}_y$ , with which it was strongly correlated. NDVI was  
35  
36 246 correlated with northing and easting, but was retained as it is a more direct measure of  
37  
38 247 seasonal primary productivity than northing or easting. Thus, nine variables were used in the  
39  
40 248 analyses (Appendix S1; Figure 1): six environmental variables (mean annual temperature,  
41  
42 249 summed annual precipitation,  $\text{NH}_x$ , soil percent organic carbon, NDVI, and dominating land-  
43  
44 250 cover class) and three geographical variables (northing, easting and altitude). While these  
45  
46 251 selected variables vary along gradients on the broad scales that are addressed in our study, it  
47  
48 252 should be noted that correlative relationships do not imply causal relationships.  
49  
50  
51  
52  
53

54 254 Data preparation  
55  
56  
57  
58  
59  
60

1  
2  
3 255 Fungal species records per latitude-longitude coordinate were summed within each  $50 \times 50$   
4  
5 256 km grid extending over Europe and matched to UTM (Universal Transverse Mercator  
6  
7 257 coordinate system; a more geographically accurate projection for both northing and easting  
8  
9 258 bounds) zone 32. Environmental data were extracted for each fungal record (to precise  
10  
11 259 latitude-longitude positions), and were then averaged within each grid cell to match the  
12  
13 260 gridded fungal data. Land cover was recorded as the CLC class with the highest number of  
14  
15 261 fungal records in each grid cell. Values for each environmental variable were originally linked  
16  
17 262 directly to each species record at the most precise spatial resolution possible; thus, the values  
18  
19 263 reported for grid cells are means for all data points found within each cell and not an overall  
20  
21 264 equal-area average across each grid cell. They are optimally predictive of environmental  
22  
23 265 conditions leading to a fruit body presence. Data were originally analysed at three spatial  
24  
25 266 resolutions ( $50 \times 50$  km,  $20 \times 20$  km and  $10 \times 10$  km), with the  $50 \times 50$  km resolution the one  
26  
27 267 that best captured large-scale compositional dynamics while being least subject to spatial bias  
28  
29 268 (Araújo, Thuiller, Williams & Reginster 2005). Geographical variables were represented by  
30  
31 269 the value of the grid cell center point.  
32  
33  
34  
35  
36

37 271 To understand temporal effects on compositional dynamics, for all taxa combined, as well as  
38  
39 272 saprotrophic and ectomycorrhizal taxa separately, the fungal data were analyzed for the whole  
40  
41 273 timespan (1970–2010) as well as for two time periods (split equally into 1970–1990 and  
42  
43 274 1991–2010). To help reduce collector biases in species representation, grid cells (grids) with  
44  
45 275 less than a total of 499 records, summed across all fungal species, were removed from the  
46  
47 276 whole time-period data set. Grids cells with less than a total of 249 records, summed across  
48  
49 277 all fungal species in the earlier time period, were removed, as were those lacking records  
50  
51 278 across both time periods. The impact of the value chosen for the minimum amount of records  
52  
53 279 within grid cells (249) was analysed during model optimization. Similar model results, or less  
54  
55  
56  
57  
58  
59  
60

1  
2  
3 280 optimal models, were obtained with number of records per grid cells of less than 4999, 2499,  
4  
5 281 999, and 249 summed records per grid (half these values for the two-time periods). The  
6  
7 282 influence of rare species was clear in grids when those with only less than 2 summed records  
8  
9 283 were removed (and inappropriate for analysis). The influence of abundantly fruiting species  
10  
11 284 was minimized by collapsing records to single units per geographical location (i.e., record  
12  
13 285 duplications were removed), though our data are populated by rarer to abundantly fruiting  
14  
15 286 taxa; hence the need for studies across fungal tissue and methodological types.”  
16  
17  
18 287

## 20 288 Statistical analyses

21  
22 289 To summarize the main gradient structure of fungal assemblage compositions, Global Non-  
23  
24 290 metric Multidimensional Scaling (GNMDS) and Detrended Correspondence Analysis (DCA)  
25  
26 291 ordinations were obtained in accordance with the multiple parallel ordination approach of van  
27  
28 292 Son and Halvorsen (2014, and references therein), using the vegan (Oksanen et al. 2013) and  
29  
30 293 MASS (Venables and Ripley 2002) packages in R. By this procedure, only ordination axes  
31  
32 294 that are extracted by both methods were accepted as important compositional gradients,  
33  
34 295 thereby ensuring that spurious axes (which may occasionally be produced by any ordination  
35  
36 296 method; Økland 1996) were not subjected to further interpretation. Many combinations of  
37  
38 297 data properties, settings, and options for the methods were explored in the initial phase of the  
39  
40 298 data analyses, including: counts, relative counts and frequencies as measures of species’  
41  
42 299 abundances in the grid cells; combined with the whole- as well as the two-time period  
43  
44 300 datasets; as well as for all, saprotrophic and ectomycorrhizal subsets of fungal communities.  
45  
46 301 GNMDS analyses with count data utilized the Bray-Curtis dissimilarity index while the  
47  
48 302 Jaccard index was used for frequency data. Each of the following settings were applied to the  
49  
50 303 count data, and the first three to relative count and frequency data, during GNMDS analyses:  
51  
52 304 no transformations or standardizations (absolute values were used), geodesic transformation,  
53  
54  
55  
56  
57  
58  
59  
60

1  
2  
3 305 Hellinger standardization, power transformation, and Wisconsin double-standardization. For  
4  
5 306 further interpretation, DCA with power-function transformed count data was selected. The  
6  
7 307 axes of these DCA's were confirmed by GNMDS by calculating pairwise correlation  
8  
9 308 coefficients between the axes. Between the models, axis 1 correlations ranged from 0.74–0.93  
10  
11 309 while axis 2 ranged from 0.23–0.82, with lowest correlation between ectomycorrhizal and  
12  
13 310 saprotrophic groups.

15  
16 311

17  
18 312 Ordination results were visualized by plotting DCA axis scores on the positions of each grid  
19  
20 313 cell. The difference between ordination scores for each of the two axes and for the two time  
21  
22 314 periods was used as the response variable in an analysis of temporal change patterns.

23  
24 315 Kendall's non-parametric correlation coefficient  $\tau$  was used to assess the significance of  
25  
26 316 environmental components in explaining community variability as represented by the DCA  
27  
28 317 axes (Supplemental Table 2). Variables that strongly correlated with one or both of the first  
29  
30 318 two DCA axes were fitted to the ordination diagram using linear regression and displayed as  
31  
32 319 either linear-termed fixed effects or cubic smooth splines (Økland 1996; Tenenbaum, De  
33  
34 320 Silva & Langford 2000; Wood 2006; Mahecha, Martínez, Lischeid & Beck 2007; Liu et al.  
35  
36 321 2008). The categorical land cover variable was analysed with the function `envfit` in `vegan` and  
37  
38 322 was found always to be significant (data not shown). The function also verified significance  
39  
40 323 of the Kendall's tau correlations for all other variables. Absolute values of  $\tau > 0.30$  were  
41  
42 324 considered substantially correlated with a DCA axis while  $\tau$  values in the interval 0.20–0.30  
43  
44 325 were considered as marginal.

46  
47  
48 326

49  
50 327 The statistical significance of the temporal difference in fungal species composition  
51  
52 328 (originating from one DCA) was assessed by three methods: paired t-tests of the individual  
53  
54 329 DCA axes scores; a multivariate paired Hotelling's T-squared test for the axes differences

1  
2  
3 330 with respect to time period; and a principal component analysis (PCA) on the matrix of  
4  
5 331 compositional change. Further PCA analyses with proportions rejected a concern that  
6  
7 332 compositional change was due to sampling bias between the two time periods. As results were  
8  
9 333 all complementary, DCA score differences were selected to be plotted geographically as a  
10  
11 334 demonstration of compositional change between the time intervals.

12  
13 335

14  
15 336 While not emphasized, as our goals concerned determining how the biogeography of fungal  
16  
17 337 assemblages related to environmental gradients, we did determine the potential that any  
18  
19 338 temporal changes in fungal assemblages were mostly the result of specific species' changes  
20  
21 339 by time (see supplemental material). Indicator species analyses were conducted on the results  
22  
23 340 of the DCA scores for each of the two time intervals, utilizing the difference in scores  
24  
25 341 between the first and second time periods for the response matrix. The species were divided  
26  
27 342 into groups by positive, negative or relatively little (no; between -0.1275–0.1275 for  
28  
29 343 saprotrophic and -0.0625–0.0625 for ectomycorrhizal groups) DCA axis score change  
30  
31 344 between the time periods. The groups were created by separating scores into equal  
32  
33 345 components of DCA score matching the color coding for figures created. Analysis was  
34  
35 346 conducted with the *indicspecies* package. All data formatting and analyses were implemented  
36  
37 347 in R version 3.2.2.

38  
39 348

#### 40 41 349 Results

42  
43 350 The primary gradients of saprotrophic and ectomycorrhizal fungal species assemblages were  
44  
45 351 both correlated with mean annual temperature (Figures 2a and 3a; Appendix S2); Kendall's  $\tau$   
46  
47 352 values were -0.55 for saprotrophic and -0.48 for ectomycorrhizal fungi. The highest  
48  
49 353 correlations for each group were for temperatures linked to cold-season measures (coldest  
50  
51 354 month or coldest quarter). Grid cells at the geographical and temperature extremes (the  
52  
53  
54  
55  
56  
57  
58  
59  
60

1  
2  
3 355 Norwegian and Alp mountain ranges) were similar with high DCA axis 1 scores, most clearly  
4  
5 356 seen for the saprotrophic fungi. In contrast, grid cells from western, coastal and low-lying  
6  
7 357 parts of Europe occurred along the opposite, low-score DCA axis 1 gradient.  
8

9 358

10  
11 359 The second compositional gradient (DCA axis 2) differed between nutritional modes. For  
12  
13 360 saprotrophic assemblages, the gradient reflected patterns related to nitrogen deposition levels  
14  
15 361 ( $\tau = -0.49$ ; Figure 2b). DCA axis 2 scores increased from central Europe to coastal areas of  
16  
17 362 the UK and Norway, which matched general nitrogen patterns (Figure 1e). In contrast, the  
18  
19 363 second assemblage gradient for ectomycorrhizal fungi separated assemblages of grid cells  
20  
21 364 from northern to central Europe (Figure 3b) and was correlated with soil organic carbon  
22  
23 365 content ( $\tau = 0.36$ ) (Figure 1c). The entire fungal community reflected similar patterns to the  
24  
25 366 saprotrophic fungi (Appendix S3; Appendix S2) and is thus not discussed further.  
26  
27

28 367

29  
30  
31 368 When separated into two time periods (1970–1990 and 1991–2010), patterns reflected those  
32  
33 369 described for the whole time period. Temperature was again the main correlate along the  
34  
35 370 primary gradient identified for saprotrophic ( $\tau = -0.51$ ) and ectomycorrhizal ( $\tau = -0.38$ )  
36  
37 371 fungal assemblages (Figure 4), with cold-season temperatures also showing high correlations  
38  
39 372 (Appendix S2). Patterns reflected those described for the whole time period. As with the  
40  
41 373 whole time period, saprotrophic fungal assemblages were separated along a second gradient  
42  
43 374 related to  $\text{NH}_x$  ( $\tau = -0.37$ ), and ectomycorrhizal fungal assemblages along a gradient related  
44  
45 375 to soil organic carbon ( $\tau = 0.37$ ) and mean annual temperature ( $\tau = -0.43$ ).  
46  
47

48 376

49  
50 377 The saprotrophic fungal assemblage gradients correlated with temperature (axis 1) and  
51  
52 378 nitrogen (axis 2). For both of the gradients, the greatest DCA score change was for grid cells  
53  
54 379 situated to the north and at higher altitudes, i.e., in the Norwegian mountain region (Figure 4  
55  
56  
57  
58  
59  
60

1  
2  
3 380 a, b). For the first, temperature-related gradient, a pattern of change was found in the opposite  
4  
5 381 direction in at least some regions of the Alps mountain range of Switzerland and Austria.  
6  
7 382 There were no robust indicator species for any of the DCA axis change groups in terms of  
8  
9 383 specificity (probability of a group based on a species' presence) and fidelity (probability of  
10  
11 384 finding a species in a group), though many species matched high specificity values (Appendix  
12  
13 385 S4). Nitrogen was similarly strongly correlated with DCA scores along the second gradient  
14  
15 386 (Appendix S2), with areas of lower nitrogen amounts tending to occupy either extreme along  
16  
17 387 the gradient. Areas in central and western Europe exhibited the least amount of temporal  
18  
19 388 change along both gradients. Though the number of grid cells was fewer for ectomycorrhizal  
20  
21 389 fungi, there was a similar trend of greatest temporal differences in assemblages at the highest  
22  
23 390 latitudes and altitudes (Figure 4 c, d). No highly matched indicator species were found for any  
24  
25 391 group, though as with the saprotrophic fungi, many species contained high specificity values  
26  
27 392 but very low fidelity values (Appendix S5).  
28  
29  
30  
31 393

## 32 394 Discussion

33  
34  
35 395 Assemblage gradients for both saprotrophic and ectomycorrhizal fungi correlated with mean  
36  
37 396 annual temperature (and collinear, cold-season temperature measures), which, as expected,  
38  
39 397 were patterned by geography and altitude. Assemblages with higher mean annual  
40  
41 398 temperatures were more similar to each other than to those at lower temperatures (Figures 2  
42  
43 399 and 3 a, c, e). Most notably, the composition of fungal assemblages in mountainous regions  
44  
45 400 were similar, regardless of whether they were situated in Norway or the Alps region of  
46  
47 401 Switzerland and Austria. If we were able to conduct the same analyses at a more precise  
48  
49 402 spatial scale that could incorporate vegetation data into the models, we expect that, in line  
50  
51 403 with earlier studies, we would find a significant relationship between the fungal and  
52  
53 404 environmental gradients, as identified with respect to fungal composition gradients, with  
54  
55  
56  
57  
58  
59  
60

1  
2  
3 405 vegetation type (e.g., Tedersoo et al. 2012; Soudzilovskaia et al. 2015; Swaty et al. 2016;  
4  
5 406 Bueno et al. 2017). A clear next challenge is to connect the fungal-environment relationships  
6  
7 407 to the fungal-vegetation relationships, ideally while simultaneously separating direct and  
8  
9 408 indirect effects from each other.

10  
11 409

12  
13 410 The second main assemblage gradient (DCA axis 2) was both different in its pattern and  
14  
15 411 varied in the main environmental correlate between the nutritional modes, though it was  
16  
17 412 relatively uniform in terms of geographic and altitudinal distribution (Figures 2 and 3 b, d, e).  
18  
19 413 The saprotrophs displayed assemblage patterns related to a gradient of N deposition, which  
20  
21 414 itself reflected oceanicity-continentality patterning, and which is a likely proxy for  
22  
23 415 anthropogenic impacts on the environment. The ectomycorrhizal pattern related to soil  
24  
25 416 organic carbon and was less geographically structured, though similar to that found by Gange  
26  
27 417 et al. (2017) in the UK. While our results cannot determine causation, different feeding  
28  
29 418 strategies may explain the correlation of nitrogen with saprotrophic fungal assemblages, and  
30  
31 419 soil organic carbon (SOC) with ectomycorrhizal fungal assemblages (Appendix S2).

32  
33 420

34  
35 421 Ectomycorrhizal fungal roles in carbon sequestration and cycling are increasingly recognized,  
36  
37 422 especially in northern latitude forests (Clemmensen et al. 2013; Averill and Hawkes 2016;  
38  
39 423 Kvaschenko, Clemmensen, Karlton & Lindahl 2017). The high correlation we found between  
40  
41 424 an assemblage composition gradient (the 2<sup>nd</sup> DCA axis) and SOC content suggests that  
42  
43 425 ectomycorrhizal fungi not only respond to, but also causally contribute to processes of  
44  
45 426 organic matter accumulation and, hence, carbon sequestration (Figure 1c, f). We effectively  
46  
47 427 captured the distributional gradation of basidiomycete taxa by vegetation type from acidic,  
48  
49 428 carbon-rich northern bogs and fens of the UK, transitioning to ectomycorrhizal dominance in  
50  
51 429 northern and mountainous forests of Scandinavia and the Alps region of Switzerland and  
52  
53  
54  
55  
56  
57  
58  
59  
60

1  
2  
3 430 Austria, on predominantly mor soils. Those locations can be contrasted with the more  
4  
5 431 continental pasturelands and woodlands containing either less woody plants or forests with  
6  
7 432 different ectomycorrhizal fungal communities and soil types. Soil pH, which is often highly  
8  
9 433 correlated with turnover in fungal community composition (Rineau and Garbaye 2009) and  
10  
11 434 implicated in fungal biogeography (Tedersoo, Bahram, Pöhlme, et al. 2014), is strongly,  
12  
13 435 negatively correlated with SOC content at a European scale (Bueno et al. 2017). SOC can also  
14  
15 436 be considered as an inverse proxy of pH. This second main compositional gradient signifies  
16  
17 437 the importance of carbon and structurally-bound compounds (and non-measured determinants  
18  
19 438 of soil carbon, e.g., vegetation and soil pH), as well as any consequential potential changes  
20  
21 439 (related to climate or land-use change) to fungi and their ecosystem services.  
22  
23

24  
25 440

26 441 Neither of the two most important ectomycorrhizal compositional gradients were strongly  
27  
28 442 correlated with nitrogen deposition amounts (a correlation of  $\tau = -0.23$  was found for the  
29  
30 443 second DCA axis; Appendix S2), which might at a first glance be surprising because effects  
31  
32 444 of N deposition on ectomycorrhizal fungal communities have been well established (Arnolds  
33  
34 445 1991; Lilleskov, Fahey & Lovett 2001; Peter, Ayer & Egli 2001; Avis, McLaughlin,  
35  
36 446 Dentinger & Reich 2003). We suggest two main explanations for this discrepancy of our  
37  
38 447 results with those of others: First, a weaker correlation means that the assemblage gradients  
39  
40 448 were structured more strongly by other factors, i.e., temperature and soil carbon, rather than  
41  
42 449 nitrogen deposition *per se*. Accordingly, our results are compatible with a considerable effect  
43  
44 450 of nitrogen deposition on fungi, but suggest interactions with carbon sequestration that have  
45  
46 451 also been shown experimentally (de Vries et al. 2009). Alternatively, the second time span  
47  
48 452 (1991–2010) might have reduced visible N impacts on assemblages, as nitrogen pollution  
49  
50 453 especially started to abate from 1994 onwards (van Strien, Boomsluiters, Noordeloos, Verweij  
51  
52 454 & Kuyper 2017). This is in accord with the reduction of N that has recently taken place in the  
53  
54  
55  
56  
57  
58  
59  
60

1  
2  
3 455 Netherlands, which has caused a marked rebound by once-affected ectomycorrhizal taxa,  
4  
5 456 especially those considered nitrogen-sensitive (nitrophobic) (van Strien et al. 2017). A  
6  
7 457 manipulative experiment testing the abatement of longer-term nitrogen addition similarly  
8  
9 458 demonstrated a re-convergence to greater community similarity with non-nitrogen enriched  
10  
11 459 treatments than those with persistent nitrogen addition (Andrew C. and Avis P., unpublished  
12  
13 460 data). Temporally dynamic environmental variables, when available, would be of further  
14  
15 461 assistance in clarifying responses, as would careful inspection between regions.  
16  
17

18 462  
19  
20 463 Interestingly, while saprotrophic fungi typically are less documented and, thus, generally  
21  
22 464 thought to exhibit less sensitivity to nitrogen deposition, the second compositional gradient  
23  
24 465 was highly correlated with nitrogen deposition (Figure 2 b, d, e). Studies of nitrogen addition  
25  
26 466 effects on saprotrophs have, however, pinpointed wood decay fungi as being susceptible  
27  
28 467 (Allison, Hanson & Treseder 2007). Community impacts of elevated nitrogen level have also  
29  
30 468 previously been found (Allison et al. 2009), though muted compared to our own results. The  
31  
32 469 molecular-based approach by those authors, covering a broader taxonomic range (at a far  
33  
34 470 smaller spatial scale), include many more taxa of the Ascomycota which, compared to macro-  
35  
36 471 fungi, are likely to be less susceptible to N. Thus, the focus on Basidiomycota and the  
37  
38 472 inclusion of wood decaying fungi in our macro-fungal data set may explain the more  
39  
40 473 pronounced community response to large-scale N content (Figure 1e). Nitrogen was also  
41  
42 474 significantly correlated with community structure when analysed across the two time intervals  
43  
44 475 (Appendix S2). Our results suggest that saprotrophic macro-fungi are an important group to  
45  
46 476 focus on in terms of nitrogen effects, with certain groups more sensitive than even  
47  
48 477 ectomycorrhizal fungi. The marginal correlation with precipitation ( $\tau = 0.27$ ) should be  
49  
50 478 further explored, as it likely represents a community gradient that reflects a response to  
51  
52 479 oceanic vs. continental climates.  
53  
54  
55  
56  
57  
58  
59  
60

1  
2  
3 480  
4

5 481 Fungal assemblage composition varied with time, but only in certain regions and with a  
6  
7 482 magnitude that varied in relation to the environmental covariates (Figure 4). The more  
8  
9 483 dramatic temperature range shift by elevation (compared to latitude), and consequent  
10  
11 484 assemblage change, appears to match the distributional patterns of plant species ranges  
12  
13 485 (Halbritter, Alexander, Edwards & Billeter 2013) and mirrors bioclimatic zonation related to  
14  
15 486 temperature (annual temperature, length of growing season). Our results indicate that fungal  
16  
17 487 assemblages in European mountain ranges are more similar, across large geographic  
18  
19 488 distances, than with those of the lowlands. This may be due to similarities in land-cover type  
20  
21 489 (Figure 1f), hosts or climatic factors themselves. Elevation structured communities differently  
22  
23 490 by latitude, for both saprotrophic and ectomycorrhizal fungi, supporting the suggestion that  
24  
25 491 the indirect effects of latitude and altitude cannot be assumed similar even if both are  
26  
27 492 structured by temperature (Halbritter et al. 2013; Grytnes et al. 2014), which also directly  
28  
29 493 affects organisms. Other factors can contribute independently to differences between each  
30  
31 494 mountain range, e.g., slope steepness, precipitation (Engler et al. 2011), and components of  
32  
33 495 biotic interactions (Pellissier et al. 2013), and could explain some of the discrepancies in  
34  
35 496 assemblage gradient changes. Relating dispersal to range shifts would also help clarify  
36  
37 497 responses (Siefert, Lesser & Fridley 2015).  
38  
39  
40  
41

42 498

43  
44 499 Greater change in assemblages occurred with saprotrophic than ectomycorrhizal fungi,  
45  
46 500 evidenced by a wider range in the difference of DCA axes scores between time periods  
47  
48 501 (Figure 4). More marked temporal-based changes in phenological responses by saprotrophic  
49  
50 502 fungi have also consistently been found, suggesting that these fungi may respond more  
51  
52 503 rapidly than ectomycorrhizal fungi, and in a variety of ways, i.e., by compositional as well as  
53  
54 504 phenological changes (Kausserud et al. 2012; Andrew et al. 2018). It would be of ecological  
55  
56  
57  
58  
59  
60

1  
2  
3 505 interest to quantify the extent to which the latter is a direct cause of the former. The degree to  
4  
5 506 which greater saprotrophic temporal change is related to management practices, forest stand  
6  
7 507 succession, or other global change components also requires further study (Bässler et al.  
8  
9 508 2010; Nordén et al. 2013; Heilmann-Clausen, Aude, et al. 2014). The effects of management  
10  
11 509 might require, however, a more precise scale resolution than that used in the current, broad-  
12  
13 510 scale study.

14  
15  
16 511

17  
18 512 Our results may serve as a platform for further macroecological research on fungi. For  
19  
20 513 example, the abiotic and biotic components of the most clearly defining biogeographical  
21  
22 514 gradients should be further examined, especially in relation to global change. We suggest  
23  
24 515 priority be given to biogeographical relationships of variables that act upon fungi in a direct  
25  
26 516 way, i.e., temperature and moisture, given how they non-additively structured fungal  
27  
28 517 assemblages, especially in terms of latitude and altitude. As mentioned earlier, it is imperative  
29  
30 518 to better connect fungi, plants and the environment, as science currently relies too often on  
31  
32 519 two-way relationships rather than a network approach capable of addressing all three main  
33  
34 520 components. Similarly, we must understand how fungal ranges, at large scales, are distributed  
35  
36 521 relative to one another as well as with respect to their hosts and/or substrates. Finally, as we  
37  
38 522 report on macro-fungal fruit bodies (as a proxy for understanding fungal assemblage patterns  
39  
40 523 overall), a primary role of which are related to reproduction and dispersal of fungi, we suggest  
41  
42 524 that adding in information on long-distance dispersal abilities – be it via spores, vegetative  
43  
44 525 structures, host or animal vectors – will help clarify the potential for movement of fungi into  
45  
46 526 new and changing habitats. These suggestions all lead to consideration of the potential for  
47  
48 527 further change of fungal communities under future global change scenarios, and what the  
49  
50 528 ecological relevance might then be.  
51  
52  
53  
54  
55  
56  
57  
58  
59  
60

1  
2  
3 529 Acknowledgements

4  
5 530 Two sources are acknowledged for financial support: The Research Council of Norway,  
6  
7 531 project “Climate change impacts on the fungal ecosystem component (ClimFun)” (11 of 38  
8  
9 532 months), and the Swiss National Science Foundation, project "Linking European Fungal  
10  
11 533 Ecology with Climate Variability” (11 months). Drs. Dag Endresen, Vegar Bakkestuen, and  
12  
13 534 Anders Nielsen we thank for open-source data acquisition. As always, our appreciation to  
14  
15 535 employees and volunteers that over the years collected, managed and provided rights to the  
16  
17 536 fungal data: the Austrian Mycological Society and Wolfgang Dämon; the Swiss national  
18  
19 537 database ([www.swissfungi.ch](http://www.swissfungi.ch)) and Peter Jakob; Deutsche Gesellschaft für Mykologie  
20  
21 538 (German Mycological Society) and Dr. Martin Schmidt; The Danish Fungal Atlas project and  
22  
23 539 Tobias Frøslev, Thomas Læssøe, Jens. H. Petersen and Jan Vesterholt; the Netherlands  
24  
25 540 Mycological Society (NMV) and A. van den Berg; the Mycological Herbarium at the Natural  
26  
27 541 History Museum (University of Oslo); the Slovenian Forestry Institute, the Central database  
28  
29 542 of fungi in Slovenia, the Slovenian Mycological Association, and Dr. Nikica Ogris;  
30  
31 543 [www.fieldmycology.net](http://www.fieldmycology.net) for support sources of the UK national database. We also  
32  
33 544 acknowledge critical and constructive comments of the editor and three anonymous  
34  
35 545 reviewers.

36  
37  
38  
39 546

40  
41 547 Data availability: All fungal and associated meta-data are provided as used for analyses in this  
42  
43 548 study and are gridded at the  $50 \times 50$  km resolution. Please see the included information on  
44  
45 549 original sources of data, or else the methods and acknowledgments sections of this  
46  
47 550 manuscript.  
48  
49  
50  
51  
52  
53  
54  
55  
56  
57  
58  
59  
60

1  
2  
3 551 References

4 552 Allison, S.D., Hanson, C.A. & Treseder, K.K. (2007). Nitrogen fertilization reduces diversity  
5 553 and alters community structure of active fungi in boreal ecosystems. *Soil Biology and*  
6  
7 554 *Biochemistry*, 39, 1878-1887.

8  
9  
10 555

11  
12  
13 556 Allison, S.D., LeBauer, D.S., Ofrecio, M.R., Reyes, R., Ta, A.M. & Tran, T.M. (2009). Low  
14 557 levels of nitrogen addition stimulate decomposition by boreal forest fungi. *Soil Biology and*  
15  
16 558 *Biochemistry*, 41, 293-302.

17  
18  
19 559

20  
21 560 Andrew, C., Heegaard, E., Kirk, P.M., Bässler, C., Heilmann-Clausen, J., Krisai-Greilhuber,  
22  
23 561 I.,... Kausrud, H. (2017). Big data integration: Pan-European fungal species observations  
24 562 assembly that addresses contemporary questions in ecology and global change biology.  
25  
26 563 *Fungal Biology Reviews*, 31, 88-98.

27  
28  
29 564

30  
31 565 Andrew, C., Heegaard, C., Gange, A.C., Senn-Irlet, B., Egli, S., Kirk, P.M.,... Boddy, L.  
32  
33 566 (2018). Congruency in fungal phenology patterns across dataset sources and scales. *Fungal*  
34  
35 567 *Ecology*, 32, 9-17.

36  
37  
38 568

39  
40 569 Araújo, M.B., Thuiller, W., Williams, P.H., & Reginster, I. (2005). Downscaling European  
41 570 species atlas distributions to a finer resolution: implications for conservation planning. *Global*  
42  
43 571 *Ecology and Biogeography*, 14, 17-30.

44  
45  
46 572

47  
48 573 Arnolds, E.E.F. (1991). Decline of ectomycorrhizal fungi in Europe. *Agriculture, Ecosystems*  
49 574 *& Environment*, 35, 209-244.

50  
51  
52 575  
53  
54  
55  
56  
57  
58  
59  
60

- 1  
2  
3 576 Averill, C., & Hawkes, C.V. (2016). Ectomycorrhizal fungi slow soil carbon cycling. *Ecology*  
4  
5 577 *Letters*, 19, 937-947.  
6  
7 578  
8  
9 579 Avis, P.G., McLaughlin, D.J., Dentinger, B.C., & Reich, P.B. (2003). Long-term increase in  
10  
11 580 nitrogen supply alters above-and below-ground ectomycorrhizal communities and increases  
12  
13 581 the dominance of *Russula* spp. in a temperate oak savanna. *New Phytologist*, 160, 239-253.  
14  
15 582  
16  
17  
18 583 Boddy, L., Buntgen, U., Egli, S., Gange, A.C., Heegaard, E., Kirk, P.M.,... Kauserud, H.  
19  
20 584 (2014). Climate variation effects on fungal fruiting. *Fungal Ecology*, 10, 20-33.  
21  
22 585  
23  
24 586 Bueno, C.G., Moora, M., Gerz, M., Davison, J., Öpik, M., Pärtel, M.,... Zobel, M. (2017).  
25  
26 587 Plant mycorrhizal status, but not type, shifts with latitude and elevation in Europe. *Global*  
27  
28 588 *Ecology and Biogeography*, 26, 690-699.  
29  
30  
31 589  
32  
33 590 Bässler, C., Müller, J., Dziöck, F., & Brandl, R. (2010). Effects of resource availability and  
34  
35 591 climate on the diversity of wood-decaying fungi. *Journal of Ecology*, 98, 822-832.  
36  
37 592  
38  
39 593 Buntgen, U., Kauserud, H., & Egli, S. (2012). Linking climate variability to mushroom  
40  
41 594 productivity and phenology. *Frontiers in Ecology and the Environment*, 10, 14-19.  
42  
43 595  
44  
45  
46 596 Clemmensen, K.E., Bahr, A., Ovaskainen, O., Dahlberg, A., Ekblad, A., Wallander, H.,...  
47  
48 597 Lindahl, B.D. (2013). Roots and associated fungi drive long-term carbon sequestration in  
49  
50 598 boreal forest. *Science*, 339, 1615-1618.  
51  
52 599  
53  
54  
55  
56  
57  
58  
59  
60

- 1  
2  
3 600 de Vries, W., Solberg, S., Dobbertin, M., Sterba, H., Laubhann, D., Van Oijen, M.,... Reinds,  
4  
5 601 G.J. (2009). The impact of nitrogen deposition on carbon sequestration by European forests  
6  
7 602 and heathlands. *Forest Ecology and Management*, 258, 1814-1823.  
8  
9 603  
10  
11 604 Dormann, C.F., Elith, J., Bacher, S., Buchmann, C., Carl, G., Carré, G.,... Münkemüller, T.  
12  
13 605 (2013). Collinearity: a review of methods to deal with it and a simulation study evaluating  
14  
15 606 their performance. *Ecography*, 36, 27-46.  
16  
17 607  
18  
19  
20 608 Engler, R., Randin, C.F., Thuiller, W., Dullinger, S., Zimmermann, N.E., Araújo, M.B.,...  
21  
22 609 Choler, P. (2011). 21st century climate change threatens mountain flora unequally across  
23  
24 610 Europe. *Global Change Biology*, 17, 2330-2341.  
25  
26 611  
27  
28  
29 612 Gange, A.C., Heegaard, E., Boddy, L., Andrew, C., Kirk, P., Halvorsen, R.,... Kauserud, H.  
30  
31 613 (2017). Trait-dependent distributional shifts in fruiting of common British fungi. *Ecography*.  
32  
33 614 40, doi: 10.1111/ecog.03233  
34  
35 615  
36  
37 616 Grytnes, J.A., Kapfer, J., Jurasinski, G., Birks, H.H., Henriksen, H., Klanderud, K.,... Birks,  
38  
39 617 H.J.B. (2014). Identifying the driving factors behind observed elevational range shifts on  
40  
41 618 European mountains. *Global Ecology and Biogeography*, 23, 876-884.  
42  
43 619  
44  
45  
46 620 Halbritter, A.H., Alexander, J.M., Edwards, P.J., & Billeter, R. (2013). How comparable are  
47  
48 621 species distributions along elevational and latitudinal climate gradients? *Global Ecology and*  
49  
50 622 *Biogeography*, 22, 1228-1237.  
51  
52 623  
53  
54  
55  
56  
57  
58  
59  
60

- 1  
2  
3 624 Halme, P., Heilmann-Clausen, J., Rämä, T., Kosonen, T., & Kunttu, P. (2012). Monitoring  
4  
5 625 fungal biodiversity—towards an integrated approach. *Fungal Ecology*, 5, 750-758.  
6  
7 626  
8  
9 627 Heilmann-Clausen, J., Barron, E.S., Boddy, L., Dahlberg, A., Griffith, G.W., Nordén, J.,...  
10  
11 628 Halme, P. (2014). A fungal perspective on conservation biology. *Conservation Biology*, 29,  
12  
13 629 61-68.  
14  
15 630  
16  
17 631 Heilmann-Clausen, J., Aude, E., Dort, K., Christensen, M., Piltaver, A., Veerkamp, M.,...  
18  
19 632 Ódor, P. (2014). Communities of wood-inhabiting bryophytes and fungi on dead beech logs  
20  
21 633 in Europe—reflecting substrate quality or shaped by climate and forest conditions? *Journal of*  
22  
23 634 *Biogeography*, 41, 2269-2282.  
24  
25 635  
26  
27 636 Heilmann-Clausen, J., Maruyama, P.K., Bruun, H.H., Dimitrov, D., Læssøe, T., Frøslev,  
28  
29 637 T.G., & Dalsgaard, B. (2016). Citizen science data reveal ecological, historical and  
30  
31 638 evolutionary factors shaping interactions between woody hosts and wood-inhabiting fungi.  
32  
33 639 *New Phytologist*, 212, 1072-1082.  
34  
35 640  
36  
37 641 Hijmans, R.J., Cameron, S.E., Parra, J.L., Jones, P.G., & Jarvis, A. (2005). Very high  
38  
39 642 resolution interpolated climate surfaces for global land areas. *International journal of*  
40  
41 643 *Climatology*, 25, 1965-1978.  
42  
43 644  
44  
45 645 Kauserud, H., Stige, L.C., Vik, J.O., Økland, R.H., Høiland, K., & Stenseth, N.C. (2008).  
46  
47 646 Mushroom fruiting and climate change. *Proceedings of the National Academy of*  
48  
49 647 *Sciences*, 105, 3811-3814.  
50  
51 648  
52  
53  
54  
55  
56  
57  
58  
59  
60

- 1  
2  
3 649 Kauserud, H., Heegaard, E., Semenov, M.A., Boddy, L., Halvorsen, R., Stige, L.C.,...  
4  
5 650 Stenseth, N.C. (2010). Climate change and spring-fruited fungi. *Proceedings of the Royal*  
6  
7 651 *Society of London B: Biological Sciences*, 277, 1169-1177.  
8  
9 652  
10  
11 653 Kauserud, H., Heegaard, E., Buntgen, U., Halvorsen, R., Egli, S., Senn-Irlet,... Høiland, K.  
12  
13 654 (2012). Warming-induced shift in European mushroom fruiting phenology. *Proceedings of*  
14  
15 655 *the National Academy of Sciences*, 109, 14488-14493.  
16  
17 656  
18  
19 657 Kyaschenko, J., Clemmensen, K.E., Karlton, E., & Lindahl, B.D. (2017). Below-ground  
20  
21 658 organic matter accumulation along a boreal forest fertility gradient relates to guild interaction  
22  
23 659 within fungal communities. *Ecology Letters*, 20, 1546–1555  
24  
25 660  
26  
27 661 Lilleskov, E.A., Fahey, T.J., & Lovett, G.M. (2001). Ectomycorrhizal fungal aboveground  
28  
29 662 community change over an atmospheric nitrogen deposition gradient. *Ecological*  
30  
31 663 *Applications*, 11, 397-410.  
32  
33 664  
34  
35 665 Liu, H.Y., Økland, T., Halvorsen, R., Gao, J.X., Liu, Q.R., Eilertsen, O., & Bratli, H. (2008).  
36  
37 666 Gradient analyses of forests ground vegetation and its relationships to environmental  
38  
39 667 variables in five subtropical forest areas, S and SW China. *Sommerfeltia*, 32, 1e196.  
40  
41 668  
42  
43 669 Mahecha, M.D., Martínez, A., Lischeid, G., & Beck, E. (2007). Nonlinear dimensionality  
44  
45 670 reduction: alternative ordination approaches for extracting and visualizing biodiversity  
46  
47 671 patterns in tropical montane forest vegetation data. *Ecological Informatics*, 2, 138e149.  
48  
49 672  
50  
51  
52  
53  
54  
55  
56  
57  
58  
59  
60

- 1  
2  
3 673 Martiny, J.B.H., Bohannan, B.J., Brown, J.H., Colwell, R.K., Fuhrman, J.A., Green, J.L.,...  
4  
5 674 Staley, J.T. (2006). Microbial biogeography: putting microorganisms on the map. *Nature*  
6  
7 675 *Reviews Microbiology*, 4, 102-112.  
8  
9 676  
10  
11 677 Meiser, A., Bálint, M., & Schmitt, I. (2014). Meta-analysis of deep-sequenced fungal  
12  
13 678 communities indicates limited taxon sharing between studies and the presence of  
14  
15 679 biogeographic patterns. *New Phytologist*, 201, 623-635.  
16  
17 680  
18  
19  
20 681 Naff, C.S., Darcy, J.L., & Schmidt, S.K. (2013). Phylogeny and biogeography of an  
21  
22 682 uncultured clade of snow chytrids. *Environmental Microbiology*, 15, 2672-2680.  
23  
24 683  
25  
26 684 Nielsen, A., Yoccoz, N.G., Steinheim, G., Storrvik, G.O., Rekdal, Y., Angeloff, M.,...  
27  
28 685 Mysterud, A. (2012). Are responses of herbivores to environmental variability spatially  
29  
30 686 consistent in alpine ecosystems?. *Global Change Biology*, 18, 3050-3062.  
31  
32 687  
33  
34  
35 688 Nordén, J., Penttilä, R., Siitonen, J., Tomppo, E., & Ovaskainen, O. (2013). Specialist species  
36  
37 689 of wood-inhabiting fungi struggle while generalists thrive in fragmented boreal forests.  
38  
39 690 *Journal of Ecology*, 101, 701-712.  
40  
41 691  
42  
43  
44 692 Oksanen, J., Blanchet, F.G., Kindt, R., Legendre, P., Minchin, P.R., O'Hara, R.B.,  
45  
46 693 Simpson, G.L., Solymos, P., Stevens, M.H.H., & Wagner, H. (2013). Vegan: Community  
47  
48 694 Ecology Package. R Package Version 2.0-9. [http://CRAN.R-project.org/](http://CRAN.R-project.org/package=vegan) package1/4vegan.  
49  
50 695  
51  
52  
53  
54  
55  
56  
57  
58  
59  
60

- 1  
2  
3 696 Pellissier, L., Pinto-Figueroa, E., Niculita-Hirzel, H., Moora, M., Villard, L., Goudet, J.,...  
4  
5 697 Guisan, A. (2013). Plant species distributions along environmental gradients: do belowground  
6  
7 698 interactions with fungi matter? *Frontiers in Plant Science*, 4, 500.  
8  
9 699  
10  
11 700 Peter, M., Ayer, F., & Egli, S. (2001). Nitrogen addition in a Norway spruce stand altered  
12  
13 701 macromycete sporocarp production and below-ground ectomycorrhizal species composition.  
14  
15 702 *New Phytologist*, 149, 311-325.  
16  
17 703  
18  
19  
20 704 Pettorelli, N., Vik, J.O., Mysterud, A., Gaillard, J.M., Tucker, C.J., & Stenseth, N.C. (2005).  
21  
22 705 Using the satellite-derived NDVI to assess ecological responses to environmental  
23  
24 706 change. *Trends in Ecology & Evolution*, 20, 503-510.  
25  
26 707  
27  
28  
29 708 Rinaldi, A.C., Comandini, O., & Kuyper, T.W. (2008). Ectomycorrhizal fungal diversity:  
30  
31 709 separating the wheat from the chaff. *Fungal Diversity*, 33, 1-45.  
32  
33 710  
34  
35 711 Rineau, F., & Garbaye, J. (2009). Effects of liming on ectomycorrhizal community structure  
36  
37 712 in relation to soil horizons and tree hosts. *Fungal Ecology*, 2, 103-109.  
38  
39 713  
40  
41 714 Siefert, A., Lesser, M.R., & Fridley, J.D. (2015). How do climate and dispersal traits limit  
42  
43 715 ranges of tree species along latitudinal and elevational gradients? *Global Ecology and*  
44  
45 716 *Biogeography*, 24, 581-593.  
46  
47 717  
48  
49  
50 718 Soudzilovskaia, N.A., Douma, J.C., Akhmetzhanova, A.A., Bodegom, P.M., Cornwell, W.K.,  
51  
52 719 Moens, E.J.,... Cornelissen, J.H. (2015). Global patterns of plant root colonization intensity  
53  
54  
55  
56  
57  
58  
59  
60

- 1  
2  
3 720 by mycorrhizal fungi explained by climate and soil chemistry. *Global Ecology and*  
4  
5 721 *Biogeography*, 24, 371-382.  
6  
7 722  
8  
9 723 Swaty, R., Michael, H.M., Deckert, R., & Gehring, C.A. (2016). Mapping the potential  
10  
11 724 mycorrhizal associations of the conterminous United States of America. *Fungal Ecology*, 24,  
12  
13 725 139-147.  
14  
15 726  
16  
17 727 Taylor, D.L., Hollingsworth, T.N., McFarland, J.W., Lennon, N.J., Nusbaum, C., & Ruess,  
18  
19 728 R.W. (2014). A first comprehensive census of fungi in soil reveals both hyperdiversity and  
20  
21 729 fine-scale niche partitioning. *Ecological Monographs*, 84, 3-20.  
22  
23 730  
24  
25 731 Tedersoo, L., Bahram, M., Toots, M., Diedhiou, A.G., Henkel, T.W., Kjøller, R.,... Polme, S.  
26  
27 732 (2012). Towards global patterns in the diversity and community structure of ectomycorrhizal  
28  
29 733 fungi. *Molecular Ecology*, 21, 4160-4170.  
30  
31 734  
32  
33 735 Tedersoo, L., & Smith, M.E. (2013). Lineages of ectomycorrhizal fungi revisited: foraging  
34  
35 736 strategies and novel lineages revealed by sequences from belowground. *Fungal Biology*  
36  
37 737 *Reviews*, 27, 83-99.  
38  
39 738  
40  
41 739 Tedersoo, L., Bahram, M., Ryberg, M., Otsing, E., Kõljalg, U., & Abarenkov, K. (2014).  
42  
43 740 Global biogeography of the ectomycorrhizal/sebacina lineage (Fungi, Sebaciniales) as  
44  
45 741 revealed from comparative phylogenetic analyses. *Molecular Ecology*, 23, 4168-4183.  
46  
47 742  
48  
49 743 Tedersoo, L., Bahram, M., Põlme, S., Kõljalg, U., Yorou, N.S., Wijesundera, R.,...  
50  
51 744 Abarenkov, K. (2014). Global diversity and geography of soil fungi. *Science*, 346, 1256688.  
52  
53  
54  
55  
56  
57  
58  
59  
60

1  
2  
3 745

4  
5 746 Tenenbaum, J.B., De Silva, V., & Langford, J.C. (2000). A global geometric framework for  
6  
7 747 nonlinear dimensionality reduction. *Science*, 290, 2319e2323.

8  
9 748

10  
11 749 Unterseher, M., Jumpponen, A.R.I., Oepik, M., Tedersoo, L., Moora, M., Dormann, C.F., &  
12  
13 750 Schnittler, M. (2011). Species abundance distributions and richness estimations in fungal  
14  
15 751 metagenomics—lessons learned from community ecology. *Molecular Ecology*, 20, 275-285.

16  
17 752

18  
19  
20 753 van Son T.C., & Halvorsen R. (2014). Multiple parallel ordinations: the importance of choice  
21  
22 754 of ordination method and weighting of species abundance data. *Sommerfeltia*, 37, 1-37.

23  
24 755

25  
26 756 van Strien, A.J., Boomsluiters, M., Noordeloos, M.E., Verweij, R.J., & Kuyper, T.W. (2017).  
27  
28 757 Woodland ectomycorrhizal fungi benefit from large-scale reduction of nitrogen deposition in  
29  
30 758 the Netherlands. *Journal of Applied Ecology*, 55, 290-298.

31  
32 759

33  
34  
35 760 Venables, W.N., & Ripley, B.D. (2002). *Modern Applied Statistics with S*, fourth ed.  
36  
37 761 Springer, New York.

38  
39 762

40  
41  
42 763 Wood, S.N. (2006). *Generalized Additive Models, an Introduction with R*. Chapman  
43  
44 764 and Hall, London.

45  
46 765

47  
48 766 Økland, R.H. (1996). Are ordination and constrained ordination alternative or complementary  
49  
50 767 strategies in general ecological studies? *Journal of Vegetation Science*, 7, 289e292.

51  
52  
53  
54  
55  
56  
57  
58  
59  
60

1  
2  
3 768 Figures legends

4  
5 769 Figure 1: Environmental covariate gridded maps displaying mean values, by geo-coordinates  
6  
7 770 linked to amount of fruit body records, for (a) mean annual temperature (degrees C), (b)  
8  
9 771 averaged total precipitation per year (mm), (c) mean percent soil organic carbon, (d) mean  
10  
11 772 NDVI, where lower values are less productive, (e) mean ammonia(-um) levels,  $\text{NH}_x$  ( $\text{kg N m}^{-2}$   
12  
13 773  $\text{s}^{-1} * 10^{-12}$ ), (f) land cover class (CLC 1), and (g) mean altitude (msl).

14  
15  
16 774

17  
18 775 Figure 2: Gradients in the composition of saprotrophic fungal communities, their  
19  
20 776 biogeographical distributions, and environmental correlates. Compositional similarities are  
21  
22 777 represented by DCA axis 1 (a, c) and axis 2 (b, d) gradients mapped onto 50x50 km grids.  
23  
24 778 Shading reflects DCA axis gradients, centered at zero (white), with darker values at either  
25  
26 779 extreme. DCA plots (e) demonstrate the influence of mean annual temperature, altitude and  
27  
28 780 nitrogen ( $\text{NH}_x$ ), all of which were highly correlated with either of the DCA axes.

29  
30  
31 781

32  
33 782 Figure 3: Gradients in the composition of ectomycorrhizal fungal communities, their  
34  
35 783 biogeographical distributions, and environmental correlates. Compositional similarities are  
36  
37 784 represented by DCA axis 1 (a, c) and axis 2 (b, d) gradients mapped onto  $50 \times 50$  km grids.  
38  
39 785 Shading reflects DCA axis gradients, centered at zero (white), with darker values at either  
40  
41 786 extreme. DCA plots (e) demonstrate the influence of mean annual temperature, altitude and  
42  
43 787 percent soil organic carbon, all of which were highly correlated with either of the DCA axes.

44  
45  
46 788

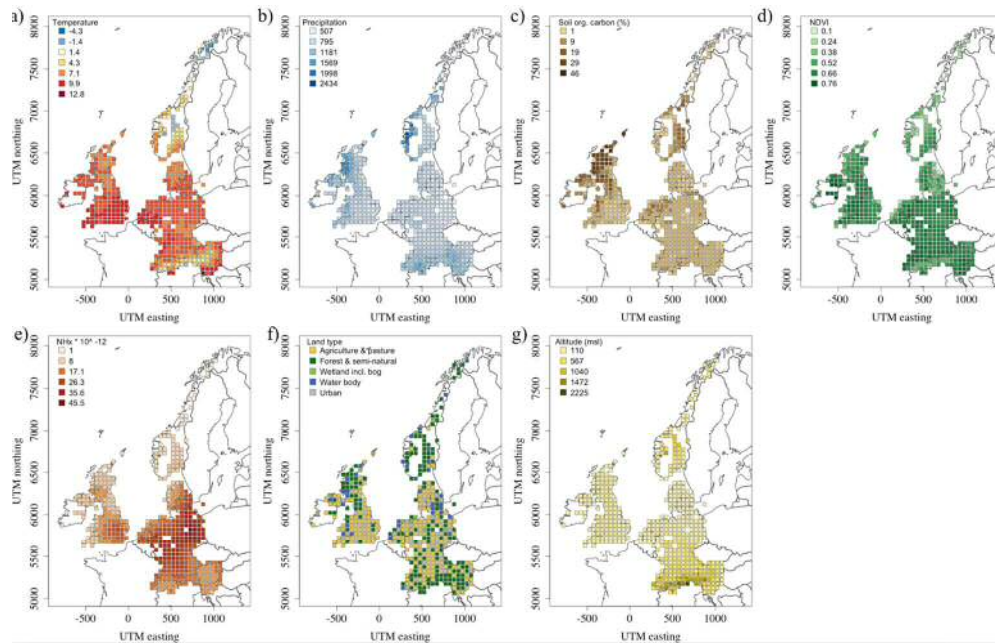
47  
48 789 Figure 4: Saprotrophic (a, b) and ectomycorrhizal (c, d) fungal community differences  
49  
50 790 between two time periods (1970-1990 vs. 1991-2010). The temporal differences of  
51  
52 791 communities by the two main DCA gradients ( $t_2 - t_1$ ) are shown mapped. All point shadings

53  
54  
55  
56  
57  
58  
59  
60

1  
2  
3  
4  
5  
6  
7  
8  
9  
10  
11  
12  
13  
14  
15  
16  
17  
18  
19  
20  
21  
22  
23  
24  
25  
26  
27  
28  
29  
30  
31  
32  
33  
34  
35  
36  
37  
38  
39  
40  
41  
42  
43  
44  
45  
46  
47  
48  
49  
50  
51  
52  
53  
54  
55  
56  
57  
58  
59  
60

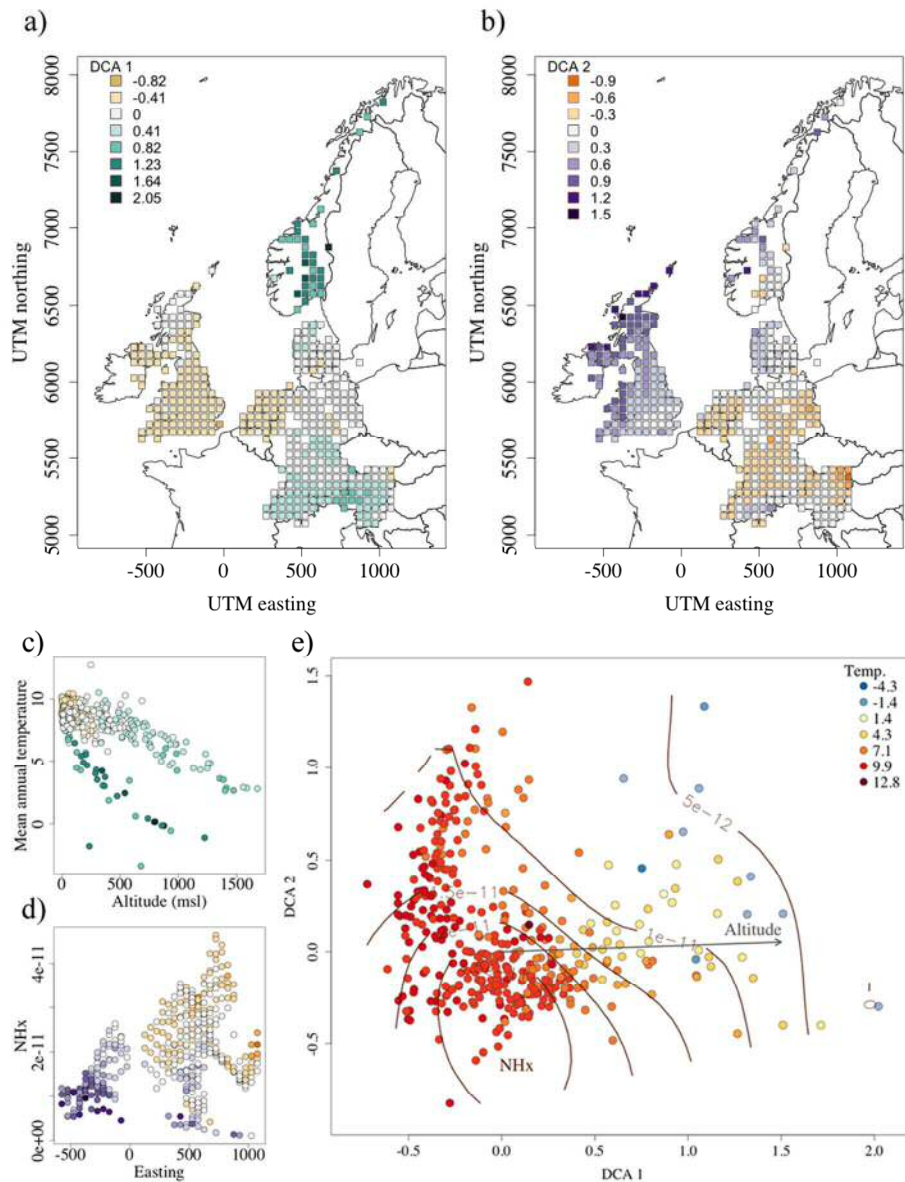
792 are centered at zero (coloured white), with shading reflecting DCA axis gradients of darker  
793 values at either extreme.

For Peer Review



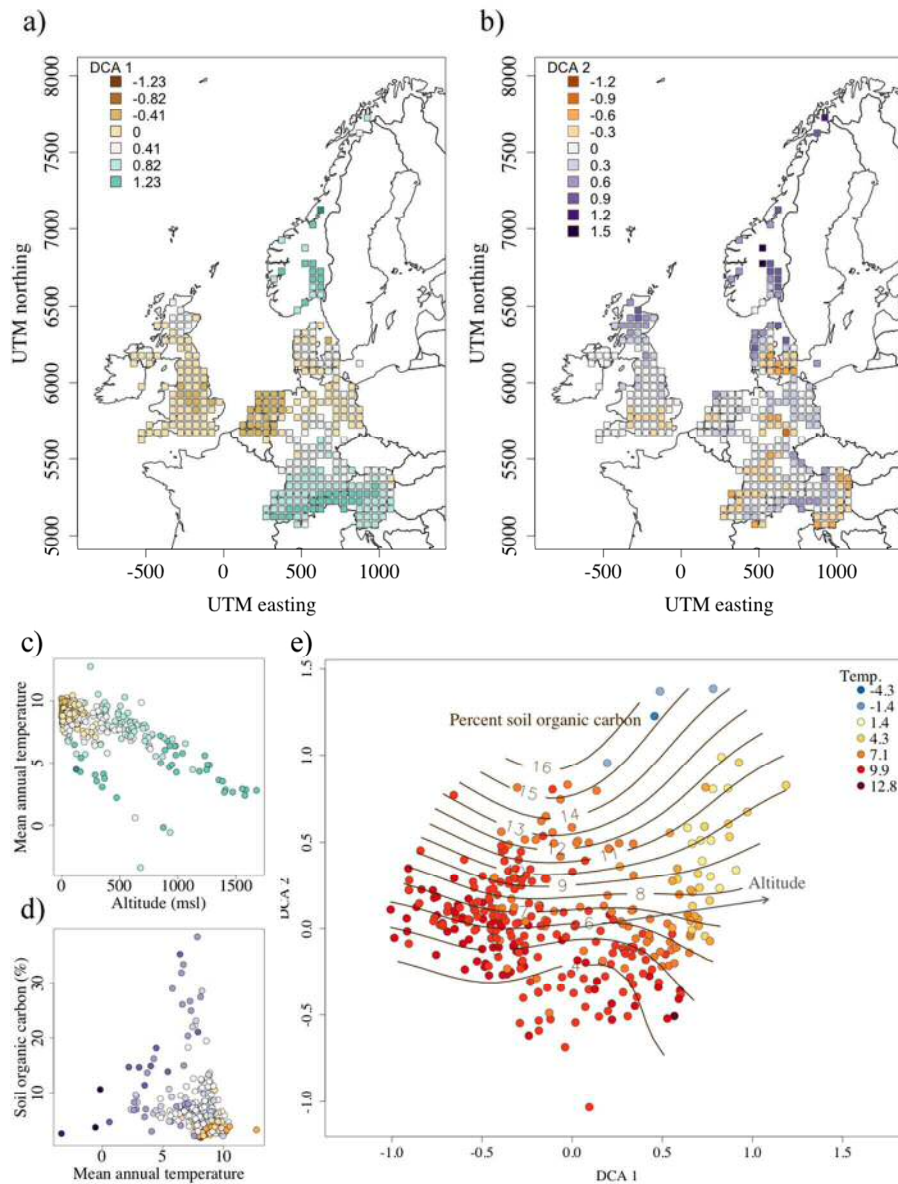
Environmental covariate gridded maps displaying mean values, by geo-coordinates linked to amount of fruit body records, for (a) mean annual temperature (degrees C), (b) averaged total precipitation per year (mm), (c) mean percent soil organic carbon, (d) mean NDVI, where lower values are less productive, (e) mean ammonia(-um) levels, NHx (kg N m<sup>-2</sup> s<sup>-1</sup> \* 10<sup>-12</sup>), (f) land cover class (CLC 1), and (g) mean altitude (msl).

243x155mm (160 x 160 DPI)



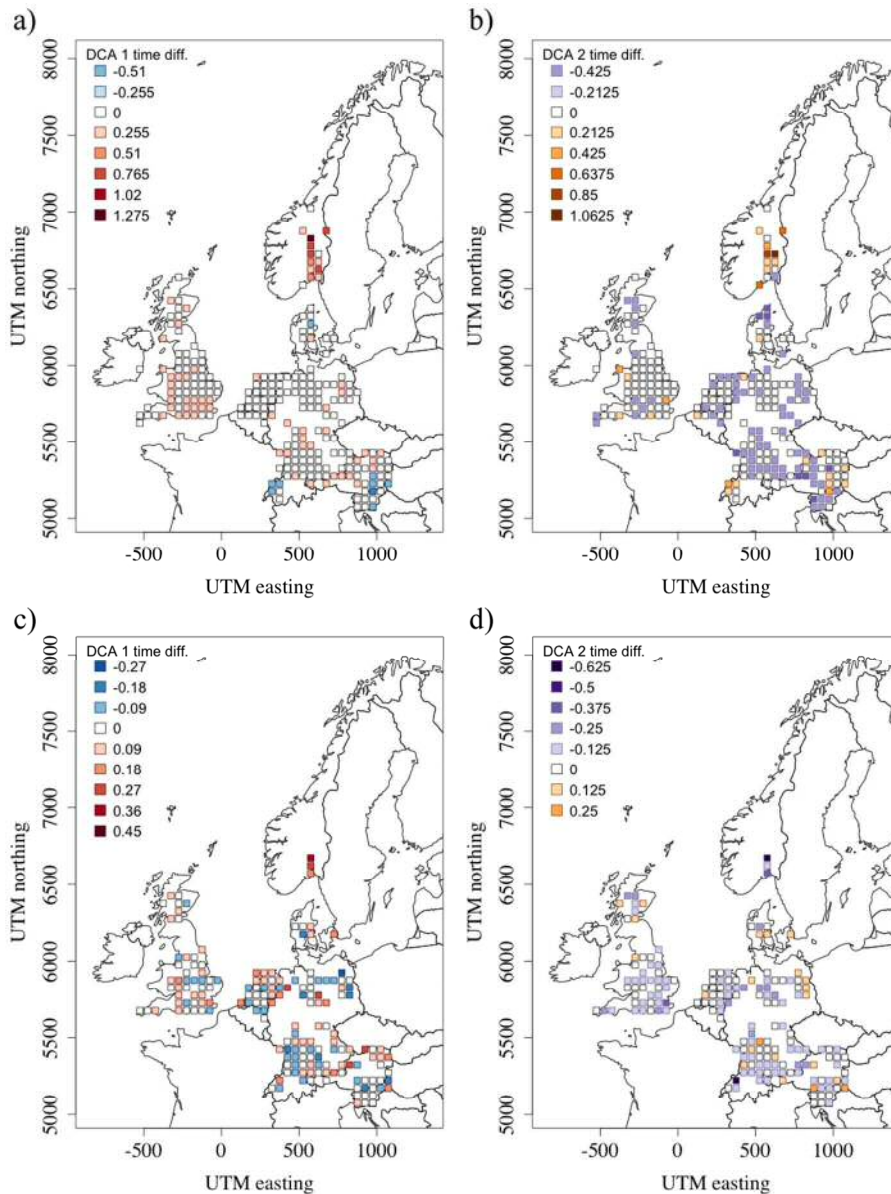
Gradients in the composition of saprotrophic fungal communities, their biogeographical distributions, and environmental correlates. Compositional similarities are represented by DCA axis 1 (a, c) and axis 2 (b, d) gradients mapped onto 50x50 km grids. Shading reflects DCA axis gradients, centered at zero (white), with darker values at either extreme. DCA plots (e) demonstrate the influence of mean annual temperature, altitude and nitrogen (NHx), all of which were highly correlated with either of the DCA axes.

400x509mm (72 x 72 DPI)



Gradients in the composition of ectomycorrhizal fungal communities, their biogeographical distributions, and environmental correlates. Compositional similarities are represented by DCA axis 1 (a, c) and axis 2 (b, d) gradients mapped onto 50 × 50 km grids. Shading reflects DCA axis gradients, centered at zero (white), with darker values at either extreme. DCA plots (e) demonstrate the influence of mean annual temperature, altitude and percent soil organic carbon, all of which were highly correlated with either of the DCA axes.

400x509mm (72 x 72 DPI)

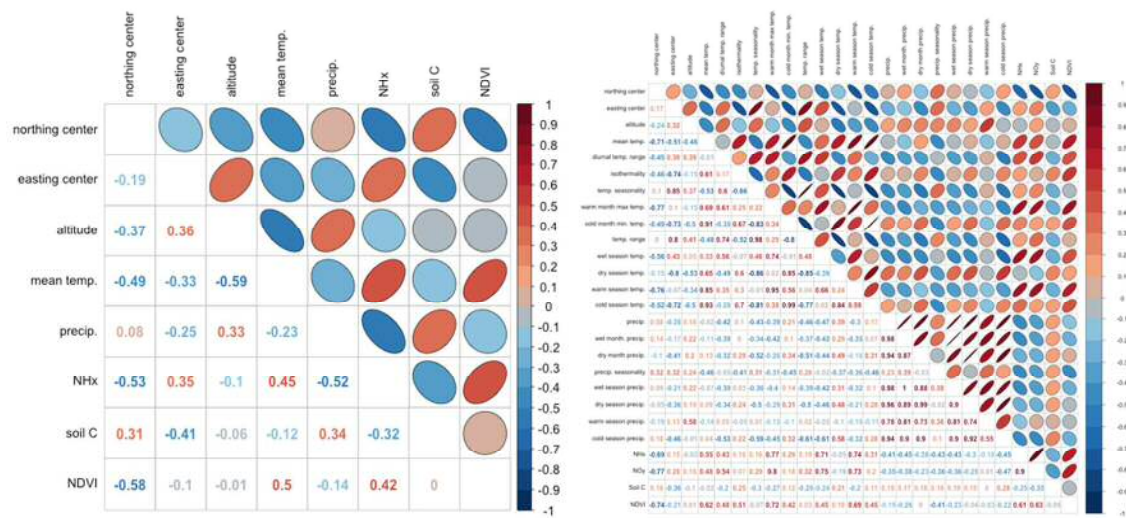


Saprotrophic (a, b) and ectomycorrhizal (c, d) fungal community differences between two time periods (1970-1990 vs. 1991-2010). The temporal differences of communities by the two main DCA gradients ( $t_2 - t_1$ ) are shown mapped. All point shadings are centered at zero (coloured white), with shading reflecting DCA axis gradients of darker values at either extreme.

400x510mm (72 x 72 DPI)

1 Continental-scale macro-fungal assemblage patterns correlate with climate, soil carbon and  
 2 nitrogen deposition

3  
 4 Carrie Andrew, Rune Halvorsen, Einar Heegaard, Thomas W Kuyper, Jacob Heilmann-  
 5 Clausen, Irmgard Krisai-Greilhuber, Claus Bässler, Simon Egli, Alan C Gange, Klaus  
 6 Høiland, Paul M Kirk, Beatrice Senn-Irlet, Lynne Boddy, Ulf Büntgen, Håvard Kausrud  
 7



8  
 9  
 10 Appendix S1: Correlation plots describing collinearity between environmental variables for  
 11 those selected as (a) the main variables in analyses as well as (b) all those available. The  
 12 correlation values are provided in the bottom left part of the graph, while pictorial  
 13 representations are found in the upper right part of the graph. Red shadings denote a positive  
 14 correlation, while blue shadings denote a negative correlation. The more linear the  
 15 relationships, i.e., the more the correlation approaches 1, the more linear the symbols. The  
 16 less linear the relationship, i.e., the more the correlation approaches 0, the more circular the  
 17 symbol shape.

1  
2  
3 1 Continental-scale macro-fungal assemblage patterns correlate with climate, soil carbon and  
4  
5 2 nitrogen deposition  
6  
7 3  
8  
9 4 Carrie Andrew, Rune Halvorsen, Einar Heegaard, Thomas W Kuyper, Jacob Heilmann-  
10  
11 5 Clausen, Irmgard Krisai-Greilhuber, Claus Bässler, Simon Egli, Alan C Gange, Klaus  
12  
13 6 Høiland, Paul M Kirk, Beatrice Senn-Irlet, Lynne Boddy, Ulf Büntgen, Håvard Kauserud  
14  
15 7  
16  
17 8 Appendix S2: Kendall tau correlations of geographical and environmental covariates with  
18  
19 9 DCA axes 1, 2 and 3 for all final models: assemblages of the whole time period and divided  
20  
21 10 into two time periods; all fungi, saprotrophic taxa only, and ectomycorrhizal taxa only.  
22  
23 11 Values above |0.30| are in bold and those above |0.40| are shaded, signifying significantly  
24  
25 12 correlated variables. The main investigated environmental correlates are in black, with  
26  
27 13 medium-grey shading for additional, collinear variables. Finally, further additional  
28  
29 14 WorldClim data variables that were not analysed any further (due to collinearity) are shaded  
30  
31 15 the lightest-grey.  
32  
33  
34  
35  
36  
37  
38  
39  
40  
41  
42  
43  
44  
45  
46  
47  
48  
49  
50  
51  
52  
53  
54  
55  
56  
57  
58  
59  
60

## 16 (worksheet 'AllWholeTime')

Variable	Axis 1	Axis 2	Axis 3	Variable	Axis 1	Axis 2	Axis 3
Northing (grid center point)	-0.07	<b>0.43</b>	-0.08	prec1	-0.08	<b>0.40</b>	-0.17
Easting (grid center point)	<b>0.41</b>	<b>-0.39</b>	0.26	prec2	0.04	0.29	-0.16
Altitude	<b>0.50</b>	-0.07	0.02	prec3	0.01	<b>0.30</b>	-0.16
Temperature (annual mean)	<b>-0.57</b>	-0.16	-0.16	prec4	0.14	0.12	-0.13
Precipitation (annual)	0.15	0.25	-0.12	prec5	0.24	-0.06	-0.03
NHx	-0.12	<b>-0.47</b>	0.19	prec6	<b>0.38</b>	-0.16	0.09
Soil Organic Carbon	0.08	0.23	0.06	prec7	<b>0.43</b>	-0.05	0.13
NDVI	-0.08	-0.20	-0.05	prec8	<b>0.34</b>	0.12	-0.02
Temperature (mean diurnal range)	0.23	<b>-0.42</b>	0.15	prec9	0.16	<b>0.34</b>	-0.14
Isothermality (diurnal/annual ranges)	<b>-0.37</b>	0.14	-0.18	prec10	0.05	<b>0.42</b>	-0.19
Temperature (seasonality)	<b>0.45</b>	<b>-0.46</b>	0.22	prec11	0.01	<b>0.38</b>	-0.22
Temperature (maximum of warmest month)	-0.03	<b>-0.59</b>	0.05	prec12	-0.05	<b>0.37</b>	-0.16
Temperature (minimum of coldest month)	<b>-0.68</b>	0.20	-0.27	tmax1	<b>-0.66</b>	0.20	-0.28
Temperature range (max. warmest month - min. coldest month)	<b>0.45</b>	<b>-0.49</b>	0.23	tmax2	<b>-0.61</b>	0.07	-0.29
Temperature (mean wettest quarter)	0.07	<b>-0.53</b>	0.18	tmax3	<b>-0.45</b>	-0.15	-0.23
Temperature (mean driest quarter)	<b>-0.49</b>	<b>0.33</b>	-0.30	tmax4	-0.20	<b>-0.39</b>	-0.06
Temperature (mean of warmest quarter)	-0.15	<b>-0.52</b>	0.03	tmax5	-0.12	<b>-0.53</b>	0.06
Temperature (mean of coldest quarter)	<b>-0.69</b>	0.18	-0.27	tmax6	-0.07	<b>-0.57</b>	0.06
Precipitation (of wettest month)	0.27	0.21	-0.10	tmax7	-0.03	<b>-0.59</b>	0.04
Precipitation (of driest month)	0.04	0.24	-0.14	tmax8	-0.08	<b>-0.58</b>	0.07
Precipitation seasonality coefficient of variation	<b>0.37</b>	0.04	0.00	tmax9	-0.18	<b>-0.52</b>	0.04
Precipitation (of wettest quarter)	0.25	0.22	-0.11	tmax10	<b>-0.45</b>	-0.30	-0.08
Precipitation (of driest quarter)	0.05	0.24	-0.14	tmax11	<b>-0.71</b>	0.08	-0.24
Precipitation (of warmest quarter)	<b>0.39</b>	-0.02	0.06	tmax12	<b>-0.68</b>	0.20	-0.27
Precipitation (of coldest quarter)	-0.03	<b>0.34</b>	-0.17	tmin1	<b>-0.68</b>	0.21	-0.27
NOy	-0.01	<b>-0.55</b>	0.26	tmin2	<b>-0.67</b>	0.16	-0.27
				tmin3	<b>-0.68</b>	0.10	-0.25
				tmin4	<b>-0.60</b>	-0.09	-0.19
				tmin5	<b>-0.38</b>	-0.29	-0.07
				tmin6	-0.29	<b>-0.30</b>	-0.06
				tmin7	-0.27	<b>-0.31</b>	-0.06
				tmin8	-0.30	-0.28	-0.05
				tmin9	<b>-0.45</b>	-0.14	-0.11
				tmin10	<b>-0.60</b>	0.02	-0.17
				tmin11	<b>-0.72</b>	0.11	-0.19
				tmin12	<b>-0.70</b>	0.22	-0.25

17

18

## 19 (worksheet 'SaproWholeTime')

Variable	Axis 1	Axis 2	Axis 3	Variable	Axis 1	Axis 2	Axis 3
Northing (grid center point)	-0.14	<b>0.34</b>	<b>-0.43</b>	prec1	-0.12	<b>0.43</b>	-0.12
Easting (grid center point)	<b>0.41</b>	<b>-0.43</b>	0.15	prec2	0.00	<b>0.32</b>	0.03
Altitude	<b>0.48</b>	-0.05	0.22	prec3	-0.03	<b>0.33</b>	-0.01
Temperature (annual mean)	<b>-0.55</b>	-0.10	0.16	prec4	0.12	0.15	0.19
Precipitation (annual)	0.13	0.27	0.02	prec5	0.25	-0.04	0.28
NHx	-0.04	<b>-0.49</b>	0.16	prec6	<b>0.41</b>	-0.16	0.23
Soil Organic Carbon	0.13	0.16	-0.16	prec7	<b>0.44</b>	-0.09	0.10
NDVI	-0.02	-0.14	0.21	prec8	<b>0.34</b>	0.10	0.08
Temperature (mean diurnal range)	0.29	<b>-0.39</b>	<b>0.31</b>	prec9	0.13	<b>0.36</b>	-0.08
Isothermality (diurnal/annual ranges)	<b>-0.36</b>	0.21	0.05	prec10	0.00	<b>0.45</b>	-0.18
Temperature (seasonality)	<b>0.48</b>	<b>-0.50</b>	0.16	prec11	-0.04	<b>0.43</b>	-0.13
Temperature (maximum of warmest month)	0.02	<b>-0.56</b>	<b>0.32</b>	prec12	-0.08	<b>0.41</b>	-0.11
Temperature (minimum of coldest month)	<b>-0.69</b>	0.25	-0.04	tmax1	<b>-0.67</b>	0.28	-0.04
Temperature range (max. warmest month - min. coldest month)	<b>0.49</b>	<b>-0.50</b>	0.18	tmax2	<b>-0.62</b>	0.16	0.07
Temperature (mean wettest quarter)	0.14	<b>-0.58</b>	0.24	tmax3	<b>-0.44</b>	-0.08	0.25
Temperature (mean driest quarter)	<b>-0.54</b>	<b>0.35</b>	-0.10	tmax4	-0.14	<b>-0.35</b>	<b>0.33</b>
Temperature (mean of warmest quarter)	-0.09	<b>-0.50</b>	0.26	tmax5	-0.05	<b>-0.52</b>	0.30
Temperature (mean of coldest quarter)	<b>-0.70</b>	0.25	-0.03	tmax6	0.00	<b>-0.55</b>	0.29
Precipitation (of wettest month)	0.26	0.20	0.03	tmax7	0.03	<b>-0.56</b>	<b>0.32</b>
Precipitation (of driest month)	0.02	0.27	0.07	tmax8	-0.02	<b>-0.56</b>	<b>0.30</b>
Precipitation seasonality coefficient of variation	<b>0.36</b>	-0.03	-0.04	tmax9	-0.12	<b>-0.48</b>	<b>0.31</b>
Precipitation (of wettest quarter)	0.24	0.21	0.03	tmax10	<b>-0.42</b>	-0.24	0.23
Precipitation (of driest quarter)	0.02	0.27	0.05	tmax11	<b>-0.71</b>	0.17	0.02
Precipitation (of warmest quarter)	<b>0.40</b>	-0.05	0.13	tmax12	<b>-0.69</b>	0.28	-0.05
Precipitation (of coldest quarter)	-0.07	<b>0.38</b>	-0.05	tmin1	<b>-0.68</b>	0.27	-0.05
NOy	0.07	<b>-0.57</b>	0.19	tmin2	<b>-0.68</b>	0.21	0.00
				tmin3	<b>-0.68</b>	0.16	0.04
				tmin4	<b>-0.58</b>	-0.03	0.13
				tmin5	<b>-0.35</b>	-0.24	0.12
				tmin6	-0.24	-0.27	0.11
				tmin7	-0.23	-0.27	0.10
				tmin8	-0.27	-0.25	0.09
				tmin9	<b>-0.43</b>	-0.09	0.03
				tmin10	<b>-0.59</b>	0.08	-0.06
				tmin11	<b>-0.71</b>	0.16	-0.05
				tmin12	<b>-0.68</b>	0.28	-0.11

20

21

22 (worksheet 'EctoWholeTime')

Variable	Axis 1	Axis 2	Axis 3	Variable	Axis 1	Axis 2	Axis 3
Nothing (grid center point)	-0.32	0.33	-0.26	prec1	-0.06	0.06	0.13
Easting (grid center point)	0.36	-0.05	-0.01	prec2	0.12	0.00	0.24
Altitude	0.60	-0.04	0.27	prec3	0.08	0.02	0.22
Temperature (annual mean)	-0.48	-0.29	-0.18	prec4	0.29	-0.10	0.28
Precipitation (annual)	0.25	0.03	0.23	prec5	0.39	-0.12	0.30
NHx	-0.10	-0.23	0.01	prec6	0.47	-0.07	0.27
Soil Organic Carbon	0.11	0.36	0.13	prec7	0.47	0.03	0.24
NDVI	0.00	-0.19	0.06	prec8	0.42	0.07	0.27
Temperature (mean diurnal range)	0.32	-0.19	0.13	prec9	0.22	0.11	0.15
Isothermality (diurnal/annual ranges)	-0.24	-0.06	0.08	prec10	0.07	0.12	0.04
Temperature (seasonality)	0.42	-0.06	-0.01	prec11	0.06	0.05	0.08
Temperature (maximum of warmest month)	0.05	-0.35	-0.07	prec12	-0.02	0.04	0.12
Temperature (minimum of coldest month)	-0.60	-0.11	-0.11	tmax1	-0.57	-0.13	-0.14
Temperature range (max. warmest month - min. coldest month)	0.47	-0.08	0.04	tmax2	-0.47	-0.21	-0.10
Temperature (mean wettest quarter)	0.11	-0.17	-0.01	tmax3	-0.30	-0.33	-0.09
Temperature (mean driest quarter)	-0.50	-0.03	-0.11	tmax4	-0.08	-0.36	-0.07
Temperature (mean of warmest quarter)	-0.09	-0.34	-0.15	tmax5	-0.05	-0.33	-0.07
Temperature (mean of coldest quarter)	-0.60	-0.13	-0.13	tmax6	0.00	-0.33	-0.10
Precipitation (of wettest month)	0.39	0.05	0.21	tmax7	0.06	-0.35	-0.07
Precipitation (of driest month)	0.14	-0.03	0.26	tmax8	-0.01	-0.35	-0.09
Precipitation seasonality coefficient of variation	0.38	0.13	0.02	tmax9	-0.09	-0.38	-0.07
Precipitation (of wettest quarter)	0.37	0.05	0.22	tmax10	-0.36	-0.35	-0.15
Precipitation (of driest quarter)	0.13	-0.02	0.26	tmax11	-0.59	-0.20	-0.16
Precipitation (of warmest quarter)	0.46	0.01	0.27	tmax12	-0.59	-0.12	-0.15
Precipitation (of coldest quarter)	0.01	0.02	0.17	tmin1	-0.61	-0.10	-0.12
NOy	0.01	-0.18	0.08	tmin2	-0.58	-0.14	-0.10
				tmin3	-0.57	-0.15	-0.09
				tmin4	-0.50	-0.25	-0.16
				tmin5	-0.34	-0.30	-0.24
				tmin6	-0.24	-0.28	-0.26
				tmin7	-0.23	-0.27	-0.26
				tmin8	-0.27	-0.25	-0.25
				tmin9	-0.42	-0.22	-0.22
				tmin10	-0.57	-0.15	-0.22
				tmin11	-0.67	-0.12	-0.17
				tmin12	-0.64	-0.09	-0.18

23

24

## 25 (worksheet 'EctoTwoTimePeriods')

Variable	Axis 1	Axis 2	Axis 3	Variable	Axis 1	Axis 2	Axis 3
Northing (grid center point)	-0.51	0.06	0.13	prec1	-0.12	0.02	0.13
Easting (grid center point)	0.41	0.08	-0.12	prec2	0.14	0.07	0.06
Altitude	0.69	0.16	-0.07	prec3	0.07	0.06	0.10
Temperature (annual mean)	-0.38	-0.43	0.12	prec4	0.41	0.06	0.02
Precipitation (annual)	0.27	0.12	0.05	prec5	0.53	0.13	-0.04
NHx	-0.08	-0.01	-0.19	prec6	0.54	0.18	-0.09
Soil Organic Carbon	0.04	0.37	0.13	prec7	0.44	0.22	-0.11
NDVI	0.19	0.01	0.04	prec8	0.45	0.23	-0.05
Temperature (mean diurnal range)	0.48	0.05	-0.08	prec9	0.19	0.10	0.05
Isothermality (diurnal/annual ranges)	-0.24	-0.09	0.12	prec10	0.02	-0.02	0.12
Temperature (seasonality)	0.45	0.11	-0.12	prec11	0.03	-0.02	0.12
Temperature (maximum of warmest month)	0.26	-0.16	-0.03	prec12	-0.04	0.02	0.14
Temperature (minimum of coldest month)	-0.54	-0.27	0.14	tmax1	-0.48	-0.30	0.14
Temperature range (max. warmest month - min. coldest month)	0.52	0.10	-0.13	tmax2	-0.38	-0.36	0.14
Temperature (mean wettest quarter)	0.17	0.01	-0.12	tmax3	-0.16	-0.41	0.12
Temperature (mean driest quarter)	-0.51	-0.19	0.20	tmax4	0.14	-0.23	0.04
Temperature (mean of warmest quarter)	0.08	-0.25	-0.02	tmax5	0.14	-0.16	-0.02
Temperature (mean of coldest quarter)	-0.52	-0.31	0.15	tmax6	0.18	-0.16	-0.02
Precipitation (of wettest month)	0.44	0.15	-0.01	tmax7	0.27	-0.16	-0.03
Precipitation (of driest month)	0.17	0.10	0.04	tmax8	0.18	-0.18	-0.02
Precipitation seasonality coefficient of variation	0.40	0.16	-0.09	tmax9	0.08	-0.24	-0.02
Precipitation (of wettest quarter)	0.43	0.14	0.00	tmax10	-0.28	-0.45	0.05
Precipitation (of driest quarter)	0.14	0.09	0.05	tmax11	-0.48	-0.38	0.12
Precipitation (of warmest quarter)	0.48	0.21	-0.09	tmax12	-0.51	-0.32	0.15
Precipitation (of coldest quarter)	-0.02	0.03	0.12	tmin1	-0.55	-0.26	0.14
NOy	-0.02	0.05	-0.13	tmin2	-0.51	-0.29	0.12
				tmin3	-0.50	-0.31	0.16
				tmin4	-0.42	-0.41	0.12
				tmin5	-0.27	-0.42	0.05
				tmin6	-0.14	-0.37	0.03
				tmin7	-0.14	-0.34	0.01
				tmin8	-0.22	-0.34	0.03
				tmin9	-0.42	-0.35	0.06
				tmin10	-0.56	-0.30	0.07
				tmin11	-0.62	-0.30	0.11
				tmin12	-0.58	-0.29	0.14

26

27

## 28 (worksheet 'SaproTwoTimePeriods')

Variable	Axis 1	Axis 2	Axis 3	Variable	Axis 1	Axis 2	Axis 3
Northing (grid center point)	-0.27	0.18	-0.45	prec1	-0.18	0.27	-0.28
Easting (grid center point)	<b>0.46</b>	<b>-0.32</b>	<b>0.37</b>	prec2	0.00	0.22	-0.09
Altitude	<b>0.55</b>	0.08	0.14	prec3	-0.05	0.23	-0.13
Temperature (annual mean)	<b>-0.51</b>	-0.02	0.11	prec4	0.19	0.15	0.11
Precipitation (annual)	0.14	0.15	-0.05	prec5	<b>0.34</b>	-0.03	0.24
NHx	-0.04	<b>-0.37</b>	0.28	prec6	<b>0.48</b>	-0.15	0.26
Soil Organic Carbon	0.21	0.01	-0.22	prec7	<b>0.45</b>	-0.18	0.16
NDVI	0.11	-0.03	0.13	prec8	<b>0.40</b>	0.00	0.05
Temperature (mean diurnal range)	<b>0.43</b>	-0.24	<b>0.37</b>	prec9	0.15	0.22	-0.19
Isothermality (diurnal/annual ranges)	<b>-0.36</b>	0.22	-0.16	prec10	-0.02	<b>0.31</b>	-0.29
Temperature (seasonality)	<b>0.55</b>	<b>-0.31</b>	<b>0.33</b>	prec11	-0.06	0.29	-0.25
Temperature (maximum of warmest month)	0.15	<b>-0.34</b>	<b>0.49</b>	prec12	-0.12	0.25	-0.23
Temperature (minimum of coldest month)	<b>-0.67</b>	0.17	-0.15	tmax1	<b>-0.64</b>	0.22	-0.16
Temperature range (max. warmest month - min. coldest month)	<b>0.58</b>	-0.30	<b>0.33</b>	tmax2	<b>-0.58</b>	0.17	-0.07
Temperature (mean wettest quarter)	0.21	<b>-0.47</b>	<b>0.40</b>	tmax3	<b>-0.36</b>	0.04	0.15
Temperature (mean driest quarter)	<b>-0.57</b>	0.24	-0.25	tmax4	0.00	-0.20	<b>0.39</b>
Temperature (mean of warmest quarter)	0.00	<b>-0.34</b>	<b>0.45</b>	tmax5	0.07	<b>-0.37</b>	<b>0.47</b>
Temperature (mean of coldest quarter)	<b>-0.66</b>	0.18	-0.14	tmax6	0.12	<b>-0.36</b>	<b>0.47</b>
Precipitation (of wettest month)	<b>0.32</b>	0.12	0.00	tmax7	0.16	<b>-0.33</b>	<b>0.49</b>
Precipitation (of driest month)	0.02	0.20	-0.06	tmax8	0.09	<b>-0.37</b>	<b>0.49</b>
Precipitation seasonality coefficient of variation	<b>0.41</b>	-0.06	0.08	tmax9	-0.03	<b>-0.32</b>	<b>0.43</b>
Precipitation (of wettest quarter)	<b>0.30</b>	0.13	0.00	tmax10	<b>-0.40</b>	-0.13	0.20
Precipitation (of driest quarter)	0.01	0.19	-0.07	tmax11	<b>-0.64</b>	0.13	-0.07
Precipitation (of warmest quarter)	<b>0.45</b>	-0.12	0.16	tmax12	<b>-0.65</b>	0.21	-0.16
Precipitation (of coldest quarter)	-0.12	0.24	-0.19	tmin1	<b>-0.67</b>	0.18	-0.16
NOy	0.05	<b>-0.47</b>	<b>0.34</b>	tmin2	<b>-0.66</b>	0.14	-0.12
				tmin3	<b>-0.65</b>	0.12	-0.07
				tmin4	<b>-0.56</b>	0.03	0.07
				tmin5	<b>-0.33</b>	-0.16	0.21
				tmin6	-0.20	-0.16	0.24
				tmin7	-0.18	-0.17	0.23
				tmin8	-0.25	-0.18	0.22
				tmin9	<b>-0.47</b>	-0.04	0.06
				tmin10	<b>-0.61</b>	0.05	-0.07
				tmin11	<b>-0.70</b>	0.09	-0.09
				tmin12	<b>-0.67</b>	0.19	-0.17

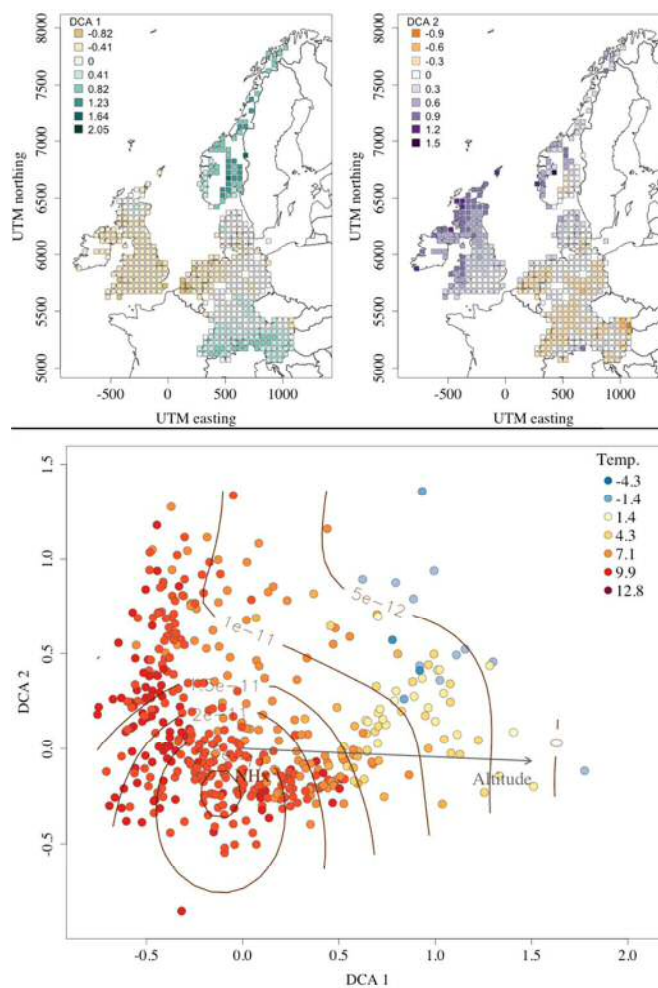
29

30

1 Continental-scale macro-fungal assemblage patterns correlate with climate, soil carbon and  
 2 nitrogen deposition

3  
 4 Carrie Andrew, Rune Halvorsen, Einar Heegaard, Thomas W Kuyper, Jacob Heilmann-  
 5 Clausen, Irmgard Krisai-Greilhuber, Claus Bässler, Simon Egli, Alan C Gange, Klaus  
 6 Høiland, Paul M Kirk, Beatrice Senn-Irlet, Lynne Boddy, Ulf Büntgen, Håvard Kausrud

7



8

9 Appendix S3: Compositional gradients and biogeographic distributions of entire fungal  
 10 communities (saprotrophic and ectomycorrhizal combined). Compositional similarities are  
 11 represented by DCA axis 1 (a) and axis 2 (b) gradients mapped onto 50x50 km grids. Shading  
 12 reflects DCA axis gradients, centered at zero (white), with darker values at either extreme. A

- 1  
2  
3 13 DCA plot (c) demonstrates the influence of mean annual temperature, altitude, and nitrogen  
4  
5 14 (NHx) on fungal community gradients.  
6  
7  
8  
9  
10  
11  
12  
13  
14  
15  
16  
17  
18  
19  
20  
21  
22  
23  
24  
25  
26  
27  
28  
29  
30  
31  
32  
33  
34  
35  
36  
37  
38  
39  
40  
41  
42  
43  
44  
45  
46  
47  
48  
49  
50  
51  
52  
53  
54  
55  
56  
57  
58  
59  
60

For Peer Review

1  
2  
3  
4  
5  
6  
7  
8  
9  
10  
11  
12  
13  
14  
15  
16  
17  
18  
19  
20  
21  
22  
23  
24  
25  
26  
27  
28  
29  
30  
31  
32  
33  
34  
35  
36  
37  
38  
39  
40  
41  
42  
43  
44  
45  
46  
47  
48  
49  
50  
51  
52  
53  
54  
55  
56  
57  
58  
59  
60

15

For Peer Review

1 Continental-scale macro-fungal assemblage patterns correlate with climate, soil carbon and  
2 nitrogen deposition

3  
4 Carrie Andrew, Rune Halvorsen, Einar Heegaard, Thomas W Kuyper, Jacob Heilmann-  
5 Clausen, Irmgard Krisai-Greilhuber, Claus Bässler, Simon Egli, Alan C Gange, Klaus  
6 Høiland, Paul M Kirk, Beatrice Senn-Irlet, Lynne Boddy, Ulf Büntgen, Håvard Kauserud

7  
8 Appendix S4: Output of saprotrophic indicator species analyses by fungal groups responding  
9 with positive (pos), relatively little (no), or negative (neg) change in DCA axis score(s)  
10 between the earlier (1970-1990) and later (1991-2010) time periods. The first and second  
11 worksheet ('DCA1', 'DCA2') are analyses conducted separately for each DCA axis. The third  
12 worksheet ('DCA1and2') conducts the analyses for the two DCA axes together. The keys for  
13 separation of DCA axis changes into groups is found in the first two worksheets.

## 14 (worksheet 'DCA1')

> summary[Indval DCA1, indvalcomp=TRUE]				### Group 1 = pos DCA1 change: 0.1275 < x	
Multilevel pattern analysis				### Group 2 = no DCA1 change: -0.1275 < x < 0.1275	
-----				### Group 3 = neg DCA1 change: x < -0.1275	
Association function: IndVal.g				## "The indicator value index is the product of two components, called 'A' and 'B'."	
Significance level (alpha): 0.05				##	
Total number of species: 3532				## Component 'A' is called the 'specificity' or 'positive predictive value' of the species as an indicator of the site group.	
Selected number of species: 50				## It is the probability that the surveyed site belongs to the target site group given the fact that the species has been found.	
Number of species associated to 1 group: 49				## If the species has a value of 1.00, this means it occurs in sites belonging to that group only.	
Number of species associated to 2 groups: 1				## Component 'B' is called the 'fidelity' or 'sensitivity' of the species as indicator of the target site group.	
List of species associated to each combination:				## It is the probability of finding the species in the sites belonging to the site group.	
				## If the species has a value less than 1.00, this means not all sites belonging to that group include that species. Only the	
				## proportion reported include that species.	
				##	
				##	
Group 1 #sps. 41					
		A B stat p-value			
Hymenochaete carpatica		0.6223 0.7778 0.696		0.002 **	
Pluteus brunneoradiatus		0.9437 0.3333 0.561		0.001 ***	
Clavaria versatilis		0.9274 0.3333 0.556		0.002 **	
Pluteus primus		0.8974 0.3333 0.547		0.003 **	
Entoloma carneogriseum		0.6958 0.3333 0.482		0.017 *	
Perenniporia japonica		1.0000 0.2222 0.471		0.002 **	
Volvariella cinerascens		1.0000 0.2222 0.471		0.003 **	
Galerina sahleri		0.9359 0.2222 0.456		0.006 **	
Aparicus abruptibulbus		0.6147 0.3333 0.453		0.010 **	
Trametes questina		0.8391 0.2222 0.432		0.015 *	
Resupinatus conspersus		0.8223 0.2222 0.427		0.014 *	
Lentinellus inolens		0.8041 0.2222 0.423		0.025 *	
Tectella patellaris		0.7818 0.2222 0.417		0.019 *	
Psilocybe turficola		0.7778 0.2222 0.416		0.016 *	
Agrocybe attenuata		1.0000 0.1111 0.333		0.039 *	
Asterotrroma medium		1.0000 0.1111 0.333		0.039 *	
Botryobasidium arachnoideum		1.0000 0.1111 0.333		0.039 *	
Ceriporia rhodella		1.0000 0.1111 0.333		0.037 *	
Chlorophyllum molybdites		1.0000 0.1111 0.333		0.037 *	
Clavaria sphagnicola		1.0000 0.1111 0.333		0.039 *	
Cystoleptia erigophora		1.0000 0.1111 0.333		0.039 *	
Fibricium subceraceum		1.0000 0.1111 0.333		0.039 *	
Galerella conocephala		1.0000 0.1111 0.333		0.037 *	
Mycenella variispora		1.0000 0.1111 0.333		0.039 *	
Panaeolus cyanescens		1.0000 0.1111 0.333		0.035 *	
Phlebia serdida		1.0000 0.1111 0.333		0.039 *	
Pholiota nameko		1.0000 0.1111 0.333		0.039 *	
Psilocybe modesta		1.0000 0.1111 0.333		0.039 *	
Resupinatus striatulus		1.0000 0.1111 0.333		0.032 *	
Sarcodontia setosa		1.0000 0.1111 0.333		0.037 *	
Stropharia umbonatescens		1.0000 0.1111 0.333		0.039 *	
Tephroclype raphanoliens		1.0000 0.1111 0.333		0.039 *	
Typhula corallina		1.0000 0.1111 0.333		0.039 *	
Galerina discreta		0.9826 0.1111 0.330		0.032 *	
Kuehneromyces vernalis		0.9826 0.1111 0.330		0.022 *	
Agrocybe farinacea		0.9741 0.1111 0.329		0.032 *	
Trichogium bifforme		0.9606 0.1111 0.327		0.028 *	
Auriculariopsis albomellea		0.4753 0.2222 0.325		0.026 *	
Arrhenia subglobispora		0.9494 0.1111 0.325		0.030 *	
Deconica micropora		0.9260 0.1111 0.321		0.016 *	
Oudemansiella ephippium		0.9037 0.1111 0.317		0.027 *	
Group 3 #sps. 8					
		A B stat p-value			
Stypella legionii		1.0000 0.1774 0.421		0.018 *	
Trechispora dimittica		0.9861 0.1613 0.399		0.023 *	
Basidioidendron spinosum		0.9646 0.1613 0.394		0.033 *	
Skeletocutis bravispora		0.9703 0.1290 0.354		0.035 *	
Flaviporus citrinellus		0.9287 0.1290 0.346		0.038 *	
Radulomyces rickii		0.9424 0.1129 0.326		0.039 *	
Entoloma		0.9356 0.1129 0.325		0.029 *	
Leptota kuehneri		0.9271 0.1129 0.324		0.046 *	
Group 1+3 #sps. 1					
		A B stat p-value			
Mycococcia nothofagi		0.9608 0.2254 0.465		0.029 *	

15

16

## 17 (worksheet 'DCA2')

> summary[Indval, DCA2, indvalcomp=TRUE]				### Group 1 = pos DCA2 change: 0.10625 <= x	
Multilevel pattern analysis				### Group 2 = no DCA2 change: -0.10625 < x < 0.10625	
-----				### Group 3 = neg DCA2 change: x < -0.10625	
Association function: Indval.g				## "The indicator value index is the product of two components, called 'A' and 'B'."	
Significance level (alpha): 0.05				## Component 'A' is called the 'specificity' or 'positive predictive value' of the species as an indicator of the site group.	
Total number of species: 3532				## It is the probability that the surveyed site belongs to the target site group given the fact that the species has been found.	
Selected number of species: 55				## If the species has a value of 1.00, this means it occurs in sites belonging to that group only.	
Number of species associated to 1 group: 40				## Component 'B' is called the 'fidelity' or 'sensitivity' of the species as indicator of the target site group.	
Number of species associated to 2 groups: 15				## It is the probability of finding the species in the sites belonging to the site group.	
List of species associated to each combination:				## If the species has a value less than 1.00, this means not all sites belonging to that group include the species. Only the proportion reported include that species.	
Group 1 #sps. 1					
	A	B	stat	p-value	
<i>Pholiota pudica</i>	0.9326	0.0641	0.245	0.037 *	
Group 3 #sps. 39					
	A	B	stat	p-value	
<i>Skeletocutis brevisparsa</i>	0.92715	0.25926	0.490	0.001 ***	
<i>Skeletocutis biguttulata</i>	0.87764	0.25926	0.477	0.001 ***	
<i>Flaviporus citrinellus</i>	0.92741	0.22222	0.454	0.001 ***	
<i>Amylocystis lapponica</i>	1.00000	0.18519	0.430	0.001 ***	
<i>Arabella sibirica</i>	1.00000	0.18519	0.430	0.001 ***	
<i>Clavaria flavipes</i>	0.89455	0.18519	0.407	0.001 ***	
<i>Jungbuhnia collabens</i>	0.96491	0.14815	0.378	0.001 ***	
<i>Xanthoporus syringae</i>	0.87424	0.14815	0.360	0.003 **	
<i>Entoloma carneogriseum</i>	0.67159	0.18519	0.353	0.010 **	
<i>Entoloma</i>	0.80745	0.14815	0.346	0.004 **	
<i>Arabella subovata</i>	1.00000	0.11111	0.333	0.002 **	
<i>Haplospilus ochraceolateritius</i>	1.00000	0.11111	0.333	0.004 **	
<i>Lepista regularis</i>	1.00000	0.11111	0.333	0.001 ***	
<i>Entoloma scabropellia</i>	0.72446	0.14815	0.328	0.014 *	
<i>Fayodia campanella</i>	0.95238	0.11111	0.325	0.005 **	
<i>Lepista multiformis</i>	0.91549	0.11111	0.319	0.004 **	
<i>Antrodia pallasi</i>	0.90909	0.11111	0.318	0.001 ***	
<i>Postia lateritia</i>	0.90909	0.11111	0.318	0.005 **	
<i>Antrodia pallascens</i>	0.88235	0.11111	0.313	0.008 **	
<i>Sistotrema raduloides</i>	0.86379	0.11111	0.310	0.003 **	
<i>Flaviporus americanus</i>	0.83333	0.11111	0.304	0.008 **	
<i>Lentinellus insidens</i>	0.71429	0.11111	0.282	0.029 *	
<i>Resupinatus conspersus</i>	0.67445	0.11111	0.274	0.038 *	
<i>Anomoporia bombycina</i>	1.00000	0.07407	0.272	0.013 *	
<i>Cabalodontia cretacea</i>	1.00000	0.07407	0.272	0.015 *	
<i>Clavaria pullei</i>	1.00000	0.07407	0.272	0.008 **	
<i>Gloeocystidiellum convolvens</i>	1.00000	0.07407	0.272	0.014 *	
<i>Ferensiporia japonica</i>	1.00000	0.07407	0.272	0.012 *	
<i>Fycnosporellus alboluteus</i>	1.00000	0.07407	0.272	0.011 *	
<i>Uncobasidium luteolum</i>	1.00000	0.07407	0.272	0.014 *	
<i>Gloeophyllum protractum</i>	0.96154	0.07407	0.267	0.021 *	
<i>Skeletocutis albocremea</i>	0.90909	0.07407	0.259	0.020 *	
<i>Diplomitoporus crustulinus</i>	0.88710	0.07407	0.256	0.018 *	
<i>Antrodia albobrunea</i>	0.86957	0.07407	0.254	0.022 *	
<i>Odontidium romellii</i>	0.85558	0.07407	0.252	0.032 *	
<i>Hyphodontia efulvata</i>	0.85246	0.07407	0.251	0.036 *	
<i>Laurilia sulcata</i>	0.84507	0.07407	0.250	0.026 *	
<i>Phlebia griseoflavescens</i>	0.80082	0.07407	0.244	0.039 *	
<i>Lentaria epichnoa</i>	0.77458	0.07407	0.240	0.042 *	
Group 1+2 #sps. 10					
	A	B	stat	p-value	
<i>Hyphoderma setigerum</i>	1.0000	0.7887	0.888	0.001 ***	
<i>Botryobasidium subconatum</i>	0.9949	0.7746	0.878	0.001 ***	
<i>Cinereomyces lindbladii</i>	0.9837	0.6526	0.801	0.003 **	
<i>Sistotrema brinkmannii</i>	0.9845	0.6479	0.799	0.001 ***	
<i>Marasmiellus vaillantii</i>	0.9664	0.6526	0.794	0.002 **	
<i>Clitocybe distreta</i>	0.9691	0.5915	0.765	0.001 ***	
<i>Pluteus thomsonii</i>	0.9447	0.5869	0.745	0.003 **	
<i>Crepidotus epibryus</i>	1.0000	0.5305	0.728	0.008 **	
<i>Hyphodontia radula</i>	0.9470	0.5023	0.690	0.003 **	
<i>Agrocybe rivulosa</i>	0.9368	0.2535	0.487	0.043 *	
Group 1+3 #sps. 3					
	A	B	stat	p-value	
<i>Mycena strobilicicola</i>	0.91694	0.20952	0.438	0.013 *	
<i>Pluteus primus</i>	0.92470	0.10476	0.311	0.047 *	
<i>Agaricus abruptibulbus</i>	0.94235	0.09524	0.300	0.037 *	
Group 2+3 #sps. 2					
	A	B	stat	p-value	
<i>Humidicutis calyptiformis</i>	0.9122	0.3827	0.591	0.001 ***	
<i>Clavaria fumosa</i>	0.9174	0.3704	0.583	0.009 **	

18

19

## 20 (worksheet 'DCA1and2')

> summary(Indval_DCAland2, indvalcomp=TRUE)			
		### Group 1 = pos DCA1, pos DCA2 change	
		### Group 2 = pos DCA1, neg DCA2 change	
Multilevel pattern analysis		### Group 3 = pos DCA1, no DCA2 change	
-----		### Group 4 = no DCA1, pos DCA2 change	
		### Group 5 = no DCA1, neg DCA2 change	
Association function: IndVal.g		### Group 6 = no DCA1, no DCA2 change	
Significance level (alpha): 0.05		### Group 7 = neg DCA1, pos DCA2 change	
		### Group 8 = neg DCA1, neg DCA2 change	
		### Group 9 = neg DCA1, no DCA2 change	
Total number of species: 3532			
Selected number of species: 36			
Number of species associated to 1 group: 36		** "The indicator value index is the product of two components, called 'A' and 'B'.	
Number of species associated to 2 groups: 0		**	
Number of species associated to 3 groups: 0		** Component 'A' is called the 'specificity' or 'positive predictive value' of the species as an indicator of the site group.	
Number of species associated to 4 groups: 0		** It is the probability that the surveyed site belongs to the target site group given the fact that the species has been found.	
Number of species associated to 5 groups: 0		** If the species has a value of 1.00, this means it occurs in sites belonging to that group only.	
Number of species associated to 6 groups: 0		**	
Number of species associated to 7 groups: 0		** Component 'B' is called the 'fidelity' or 'sensitivity' of the species as indicator of the target site group.	
Number of species associated to 8 groups: 0		** It is the probability of finding the species in the sites belonging to the site group.	
		** If the species has a value less than 1.00, this means not all sites belonging to that group include the species. Only the	
List of species associated to each combination:		** proportion reported include that species.	
		**	
Group 1 #sps. 7			
	A	B	stat p-value
Amylocystis lapponica	0.9088	0.3077	0.529 0.044 *
Athelia sibirica	0.7292	0.3077	0.474 0.046 *
Anomopora bombycina	1.0000	0.1538	0.392 0.021 *
Clavaria pulvis	1.0000	0.1538	0.392 0.019 *
Pycnoporellus albuluteus	1.0000	0.1538	0.392 0.023 *
Uncobasidium luteolum	1.0000	0.1538	0.392 0.018 *
Gloeophyllum protractum	0.9122	0.1538	0.375 0.049 *
Group 7 #sps. 4			
	A	B	stat p-value
Perenniporia japonica	1.0000	0.2857	0.535 0.022 *
Galerina discreta	0.9787	0.1429	0.374 0.047 *
Agrocybe farinacea	0.9683	0.1429	0.372 0.047 *
Arrhenia subglobispora	0.9386	0.1429	0.366 0.047 *
Group 8 #sps. 5			
	A	B	stat p-value
Deconica micropora	0.9819	1.0000	0.991 0.001 ***
Antrodiaella leucomantha	0.9286	1.0000	0.964 0.020 *
Wycosa juniperina	0.9242	1.0000	0.961 0.021 *
Macronella flava	0.8861	1.0000	0.941 0.002 **
Entoloma callichroum	0.8726	1.0000	0.934 0.032 *
Group 9 #sps. 20			
	A	B	stat p-value
Ceriporia rhodella	1.0000	1.0000	1.000 0.008 **
Galerella conocephala	1.0000	1.0000	1.000 0.008 **
Sarcodontia setosa	1.0000	1.0000	1.000 0.008 **
Kuehneromyces vernalis	0.9940	1.0000	0.997 0.002 **
Delicatula cuspidata	0.9907	1.0000	0.995 0.005 **
Trichaptum bifforme	0.9889	1.0000	0.994 0.002 **
Gymnopus exsculptus	0.9821	1.0000	0.991 0.008 **
Maireina maxima	0.9727	1.0000	0.986 0.011 *
Oudemansiella ephippium	0.9690	1.0000	0.984 0.003 **
Hymenochaete mougentii	0.9649	1.0000	0.982 0.009 **
Clitocybe discolor	0.9316	1.0000	0.965 0.018 *
Clitocybe infundibuliformis	0.9242	1.0000	0.961 0.016 *
Hygrocybe murinaea	0.9167	1.0000	0.957 0.014 *
Crepidotus brunneoroseus	0.9016	1.0000	0.950 0.015 *
Trametes quercina	0.8948	1.0000	0.946 0.015 *
Volvariella cinnamascens	0.8750	1.0000	0.935 0.018 *
Fluxus insidiosus	0.8747	1.0000	0.935 0.006 **
Pholiota pudica	0.8730	1.0000	0.934 0.028 *
Melanoleuca subsejuncta	0.8594	1.0000	0.927 0.023 *
Clavaria vermatilis	0.8228	1.0000	0.907 0.028 *

21

22

1 Continental-scale macro-fungal assemblage patterns correlate with climate, soil carbon and  
2 nitrogen deposition

3  
4 Carrie Andrew, Rune Halvorsen, Einar Heegaard, Thomas W Kuyper, Jacob Heilmann-  
5 Clausen, Irmgard Krisai-Greilhuber, Claus Bässler, Simon Egli, Alan C Gange, Klaus  
6 Høiland, Paul M Kirk, Beatrice Senn-Irlet, Lynne Boddy, Ulf Büntgen, Håvard Kausrud

7  
8 Appendix S5: Output of ectomycorrhizal indicator species analyses by fungal groups  
9 responding with positive (pos), relatively little (no), or negative (neg) change in DCA axis  
10 score(s) between the earlier (1970-1990) and later (1991-2010) time periods. The first and  
11 second worksheet ('DCA1', 'DCA2') are analyses conducted separately for each DCA axis.  
12 The third worksheet ('DCA1and2') conducts the analyses for the two DCA axes together. The  
13 keys for separation of DCA axis changes into groups is found in the first two worksheets.

14  
15 (worksheet 'DCA1')

```

> summary(indval DCA1, indvalcomp=TRUE)
##### Group 1 = pos DCA1 change; 0.045 <= x
##### Group 2 = no DCA1 change; -0.045 < x < 0.045
##### Group 3 = neg DCA1 change; x < -0.045
-----
## "The indicator value index is the product of two components, called 'A' and 'B'."
##
Association function: IndVal.g
Significance level (alpha): 0.05
## Component 'A' is called the 'specificity' or 'positive predictive value' of the species as an indicator of the site group.
## It is the probability that the surveyed site belongs to the target site group given the fact that the species has been found.
Total number of species: 2013
## If the species has a value of 1.00, this means it occurs in sites belonging to that group only.
Selected number of species: 9
##
Number of species associated to 1 group: 5
## Component 'B' is called the 'fidelity' or 'sensitivity' of the species as indicator of the target site group.
Number of species associated to 2 groups: 4
## It is the probability of finding the species in the sites belonging to the site group.
## If the species has a value less than 1.00, this means not all sites belonging to that group include the species. Only the
List of species associated to each combination:
## proportion reported include that species.
##
Group 1 #sps. 1
      A      B stat p.value
Cortinarius camptoron 0.82174 0.07317 0.245 0.046 *
-----
Group 2 #sps. 1
      A      B stat p.value
Russula pseudoromellii 1.00000 0.1029 0.321 0.005 **
-----
Group 3 #sps. 3
      A      B stat p.value
Amanita betulae 1.00000 0.06349 0.252 0.035 *
Cortinarius humolens 1.00000 0.06349 0.252 0.016 *
Sarcodon lundellii 1.00000 0.06349 0.252 0.049 *
-----
Group 1+2 #sps. 1
      A      B stat p.value
Sebacina grisea 0.9173 0.4128 0.615 0.003 **
-----
Group 2+3 #sps. 3
      A      B stat p.value
Russula luteotacta 0.9914 0.5496 0.738 0.002 **
Russula subfoetens 0.9867 0.5496 0.736 0.001 ***
Phellodon niger 0.9063 0.5191 0.686 0.005 **
---

```

16

17

18 (worksheet 'DCA2')

> summary(indval DCA2, indvalcomp=TRUE)			
Multilevel pattern analysis		### Group 1 = pos DCA2 change: 0.0625 < x	
		### Group 2 = no DCA2 change: -0.0625 < x < 0.0625	
		### Group 3 = neg DCA2 change: x < -0.0625	
-----			
Association function: IndVal.g		## "The indicator value index is the product of two components, called 'A' and 'B'.	
Significance level (alpha): 0.05		## Component 'A' is called the 'specificity' or 'positive predictive value' of the species as an indicator of the site group.	
Total number of species: 2013		## It is the probability that the surveyed site belongs to the target site group given the fact that the species has been found.	
Selected number of species: 7		## If the species has a value of 1.00, this means it occurs in sites belonging to that group only.	
Number of species associated to 1 group: 6		## Component 'B' is called the 'fidelity' or 'sensitivity' of the species as indicator of the target site group.	
Number of species associated to 2 groups: 1		## It is the probability of finding the species in the sites belonging to the site group.	
List of species associated to each combination:		## If the species has a value less than 1.00, this means not all sites belonging to that group include the species. Only the	
		## proportion reported include that species.	
Group 1 #sps. 1	A	B	stat p.value
Neoboletus pseudosulphureus	1.00000	0.07407	0.272 0.045 *
Group 3 #sps. 5	A	B	stat p.value
Tomentella atroarenicolor	0.67244	0.13636	0.303 0.042 *
Cortinarius squilanus	1.00000	0.09091	0.302 0.015 *
Tomentellopsis pusilla	1.00000	0.09091	0.302 0.018 *
Russula innocua	0.94848	0.09091	0.294 0.015 *
Hebeloma eburneum	0.87588	0.09091	0.282 0.036 *
Group 1+2 #sps. 1	A	B	stat p.value
Cortinarius splendens	0.9660	0.3933	0.616 0.023 *
---			

19

20 (worksheet 'DCA1and2')

> summary(indval DCA1and2, indvalcomp=TRUE)			
Multilevel pattern analysis		### Group 1 = pos DCA1, pos DCA2 change	
		### Group 2 = pos DCA1, neg DCA2 change	
		### Group 3 = pos DCA1, no DCA2 change	
		### Group 4 = no DCA1, pos DCA2 change	
		### Group 5 = no DCA1, neg DCA2 change	
		### Group 6 = no DCA1, no DCA2 change	
		### Group 7 = neg DCA1, pos DCA2 change	
		### Group 8 = neg DCA1, neg DCA2 change	
		### Group 9 = neg DCA1, no DCA2 change	
-----			
Association function: IndVal.g		## "The indicator value index is the product of two components, called 'A' and 'B'.	
Significance level (alpha): 0.05		## Component 'A' is called the 'specificity' or 'positive predictive value' of the species as an indicator of the site group.	
Total number of species: 2013		## It is the probability that the surveyed site belongs to the target site group given the fact that the species has been found.	
Selected number of species: 25		## If the species has a value of 1.00, this means it occurs in sites belonging to that group only.	
Number of species associated to 1 group: 25		## Component 'B' is called the 'fidelity' or 'sensitivity' of the species as indicator of the target site group.	
Number of species associated to 2 groups: 0		## It is the probability of finding the species in the sites belonging to the site group.	
Number of species associated to 3 groups: 0		## If the species has a value less than 1.00, this means not all sites belonging to that group include the species. Only the	
Number of species associated to 4 groups: 0		## proportion reported include that species.	
Number of species associated to 5 groups: 0		##	
Number of species associated to 6 groups: 0		##	
Number of species associated to 7 groups: 0		##	
Number of species associated to 8 groups: 0		##	
List of species associated to each combination:		##	
		##	
Group 1 #sps. 24	A	B	stat p.value
Cortinarius squilanus	1.0000	0.5000	0.707 0.001 ***
Faxillus velidus	0.7941	0.5000	0.630 0.001 ***
Faxillus obscurisporus	0.7343	0.5000	0.606 0.005 **
Cortinarius collinitoides	1.0000	0.2500	0.500 0.022 *
Cortinarius violaceipes	1.0000	0.2500	0.500 0.022 *
Descolea antarctica	1.0000	0.2500	0.500 0.028 *
Hebeloma vesterholtii	1.0000	0.2500	0.500 0.022 *
Tretomyces lutescens	1.0000	0.2500	0.500 0.028 *
Hebeloma album	0.9444	0.2500	0.486 0.011 *
Cortinarius pseudosolor	0.8889	0.2500	0.471 0.012 *
Cortinarius variiformis	0.8706	0.2500	0.467 0.015 *
Cortinarius rhizophorus	0.8621	0.2500	0.464 0.031 *
Hebeloma quecatorum	0.8055	0.2500	0.450 0.007 **
Cortinarius lilacinovelatus	0.8065	0.2500	0.449 0.046 *
Cortinarius americanus	0.8003	0.2500	0.447 0.028 *
Cortinarius multiiformis	0.7931	0.2500	0.445 0.027 *
Lactarius terenopus	0.7887	0.2500	0.444 0.030 *
Cortinarius lepidoides	0.7576	0.2500	0.435 0.041 *
Inocybe melanopoda	0.7368	0.2500	0.429 0.038 *
Cortinarius tilliaceus	0.7164	0.2500	0.423 0.024 *
Cortinarius selandicus	0.6757	0.2500	0.411 0.041 *
Tricholoma inocyboides	0.6667	0.2500	0.408 0.031 *
Sebacina laciniata	0.6588	0.2500	0.406 0.039 *
Ramaria kriegsteineri	0.6538	0.2500	0.404 0.040 *
Group 7 #sps. 1	A	B	stat p.value
Tomentellopsis pusilla	1.0	0.2	0.447 0.042 *
---			

21